



Continuous Plant-Based and Remote Sensing for Determination of Fruit Tree Water Status

Alessandro Carella * , Pedro Tomas Bulacio Fischer , Roberto Massenti and Riccardo Lo Bianco *

Department of Agricultural, Food and Forest Sciences (SAAF), University of Palermo, 90128 Palermo, Italy; pedrotomas.bulaciofischer@unipa.it (P.T.B.F.); roberto.massenti@unipa.it (R.M.)

* Correspondence: alessandro.carella@unipa.it (A.C.); riccardo.lobianco@unipa.it (R.L.B.)

Abstract: Climate change poses significant challenges to agricultural productivity, making the efficient management of water resources essential for sustainable crop production. The assessment of plant water status is crucial for understanding plant physiological responses to water stress and optimizing water management practices in agriculture. Proximal and remote sensing techniques have emerged as powerful tools for the non-destructive, efficient, and spatially extensive monitoring of plant water status. This review aims to examine the recent advancements in proximal and remote sensing methodologies utilized for assessing the water status, consumption, and irrigation needs of fruit tree crops. Several proximal sensing tools have proved useful in the continuous estimation of tree water status but have strong limitations in terms of spatial variability. On the contrary, remote sensing technologies, although less precise in terms of water status estimates, can easily cover from medium to large areas with drone or satellite images. The integration of proximal and remote sensing would definitely improve plant water status assessment, resulting in higher accuracy by integrating temporal and spatial scales. This paper consists of three parts: the first part covers current plant-based proximal sensing tools, the second part covers remote sensing techniques, and the third part includes an update on the combined use of the two methodologies.

Keywords: proximal sensors; irrigation scheduling; precision irrigation; internet of things; UAV; satellite; vegetation index



Citation: Carella, A.; Bulacio Fischer, P.T.; Massenti, R.; Lo Bianco, R. Continuous Plant-Based and Remote Sensing for Determination of Fruit Tree Water Status. *Horticulturae* **2024**, *10*, 516. <https://doi.org/10.3390/horticulturae10050516>

Academic Editors: Georgios Koubouris and Arturo Alvinio

Received: 1 March 2024

Revised: 8 May 2024

Accepted: 13 May 2024

Published: 16 May 2024



Copyright: © 2024 by the authors. Licensee MDPI, Basel, Switzerland. This article is an open access article distributed under the terms and conditions of the Creative Commons Attribution (CC BY) license (<https://creativecommons.org/licenses/by/4.0/>).

1. Introduction

The world's sustainable supply of water resources has become a critically important issue in the context of recent environmental and agricultural challenges. Agriculture, as one of the main water-consuming sectors, plays a crucial role in the responsible management of global water resources [1–4]. Climate change-induced temperature rises impact water availability through increased evapotranspiration and subsequent alterations in rainfall and river flows, increasing the frequency and intensity of heatwaves and drought events [5–7]. Therefore, understanding plant responses to water availability in order to increase their water use efficiency is becoming more and more urgent [8].

For irrigation scheduling, monitoring environmental parameters to calculate crop evapotranspiration (ET_c) has been one of the most widely used methods. It is obtained by considering a reference evapotranspiration (ET_0) and crop coefficients (K_c). The ET_c can easily be estimated following the FAO-56 method described by Allen et al. (1998) [9–11]. Nevertheless, different studies have highlighted that this method might overestimate the irrigation needed for the optimal yield and consequently diminish orchard water use efficiency [12,13], because it does not take into account the actual plant water status (PWS). In recent years, soil-based systems have been developed by using soil water potential or volumetric water content principles [14]. This includes the use of precision instruments such as tensiometers [15,16], soil psychrometers [17,18], continuous and real-time sensors [19,20], and remote sensing techniques [21,22] capable of measuring soil moisture.

However, soil-based methods could be significantly influenced by different variables such as the soil texture, and soil moisture level indirectly influences the PWS rather than measuring it directly on the plant [23]. Furthermore, we should point out that the plant is the intermediate component in the soil–plant–atmosphere continuum, and its water status is directly affected by changes in its leaf water content and leaf and stem water potential [10,24–26]. For these reasons, recently, the focus has shifted to the direct assessment of PWS.

Traditional systems for the plant-based monitoring of PWS include measurement of the stem (Ψ_{stem}) and leaf (Ψ_{leaf}) water potential using Scholander’s pressure chamber. This represents the most common method of measuring plant water potential, used as an accurate indicator of fruit trees’ water status [27,28]. However, assessing water potential using a pressure chamber is an invasive and labor-intensive procedure, requiring a skilled operator to consistently apply and release pressure to the chamber containing the leaf sample, and the operator must meticulously determine the pressure at which water emerges from the leaf petiole [29]. In addition, it could also be influenced by the osmotic component, i.e., a lower water potential may indicate lower hydration or a higher concentration of solutes, thus decreasing the osmotic potential and consequently the water potential [30]. Leaf relative water content (RWC) could also be considered a valid method for estimating PWS [31,32]. RWC quantifies the amount of water within leaf tissues relative to the maximum amount of water the leaf tissues can retain when fully hydrated. In addition, with respect to stem and leaf water potential, it takes into account some physiological phenomena such as osmotic adjustment. This is one of the mechanisms that plants use to maintain cell hydration. Consequently, the RWC remains relatively high even under water stress conditions, inducing improved cellular hydration and enhancing the ability of the plant to survive under severe water stress conditions [9,26,33]. Despite the potential reliability and relative easiness of RWC as a method for assessing PWS, similarly to determining the water potential with a pressure chamber, it is an invasive and very time-consuming method, mainly due to the need to obtain and weigh fully saturated and dry samples [34]. An alternative conventional method to assess plant water status can be the measurement of gas exchange (e.g., stomatal conductance— g_s), since it is well known that stomatal opening and closing depends on PWS, with responses differing from crop to crop [35,36]. Similar to the previous methods, these techniques are also time-consuming and require the use of expensive instruments (e.g., porometer). Other useful approaches for PWS assessment may involve indirect estimation methods such as the leaf turgor [29] and thickness [37], sap flow [38,39], stem [40,41], and fruit diameter [42]. Nonetheless, these measurements require high precision that is only achievable with the use of sensors and other precision technologies.

In recent years, the focus has moved to two new approaches for irrigation management. The first involves the use of large-scale imagery from above using instruments such as drones (UAVs) and satellites (remote sensing). The second involves the use of plant-based ground sensors to obtain more accurate data (proximal sensing) [26]. The main advantage of ground-based sensors is that they may provide continuous and real-time PWS indications, as opposed to traditional methods. The possibility of having real-time estimates of PWS and consumption greatly facilitates the grower’s decision to act at the right time with the right irrigation volume. Having precise information about the timing and volume of irrigation would allow action only when necessary, avoiding waste and thus significantly increasing water use efficiency. Consequently, there would be a positive impact in terms of sustainability from both economic and environmental perspectives.

Last-generation sensors allow accessing data directly from home via cloud, easing the farm workload. These kinds of systems belong to Internet of Things (IoTs) technologies [43]. IoTs technology mainly focuses on providing many small, interconnected devices using WSN (Wireless Sensor Network) technology [44]. With the help of WSN technologies, growers will be able to consult weather conditions, soil conditions, and plant physiological parameters collected from their farm, thus obtaining an efficient decision support system

(DSS) [45]. An evaluation issue may arise due to potential small errors introduced by the installation of sensors in sample plants. These errors could be associated with different variables, including the soil texture, soil chemical composition, presence of pathogens, etc. Remote sensing technologies, on the other hand, by providing images of entire plot areas, allow us to have data from different types of optical sensors (RGB, multispectral, thermal, hyperspectral, etc.) to assess spatial variability in terms of the health, nutrient, and water status of trees and soil [46]. The combined use of proximal and remote sensing could provide more complete and precise information on PWS since, with proximal sensors, we have accurate, continuous real-time data concerning individual plants, while data from UAVs or satellites may expand the information throughout the field [47]. In other words, there is a higher level of accuracy because of the possibility of integrating information at the temporal (proximal sensing) and spatial (remote sensing) scales. To do this clearly, appropriate models have to be developed, and exploiting machine learning techniques seems the best way to go [44,48].

On this basis, this review aims to gather state-of-the-art updates covering the use of proximal sensors, remote sensing, and the combined use of both techniques to assess the water status, consumption, and requirements of fruit tree crops. More specifically, we reviewed stem-, leaf-, and fruit-mounted sensors, the use of satellites and UAVs with multispectral, thermal, and hyperspectral sensing devices, and their combined use. In detail, this review provides an extensive overview of various proximal and remote sensors, elucidating their respective advantages, disadvantages, and practical applications. Each sensor type is carefully evaluated, offering insights into their specific capabilities and limitations when employed for assessing water status, consumption, and requirements in fruit tree crops. Following this comprehensive evaluation, this review will conclude by outlining future perspectives. Based on the insights from the analysis, this review will propose hypotheses regarding the development of efficient systems that integrate both proximal and remote sensing techniques. Ultimately, these hypotheses will foster exploration of novel approaches and methodologies for enhancing the assessment of the water status, consumption, and requirements of fruit tree crops.

2. Proximal Sensing

2.1. Leaf-Mounted Sensors

2.1.1. Leaf Patch Clamp Pressure Probe

The force exerted by water toward the cell walls of plant cells is known as leaf turgor pressure. This force is closely dependent on the water status of various parts of the plant, most notably the leaf [49]. When the plant is well-hydrated, the water inside the leaf cells tends to exert adequate pressure toward the walls. Conversely, when the plant begins to dehydrate, the cells will start losing turgor pressure and the leaf will tend to wilt [10,50]. The loss of turgor pressure is directly related to stomatal closure and a decrease in the transpiration rate [51]. Hence, leaf water status can be assessed by measuring the amount and rate of turgor pressure loss at solar noon (when the transpiration rate is highest) and the duration required for its restoration in the afternoon [52].

Early attempts to measure cell turgor include that of Green and Stanton who, in 1967, used, in *Nitella axillaris* cells, a small capillary fused at the end with the other resembling the tip of a syringe needle. This capillary contained a gas in order to act as a micromanometer [53]. A *Nitella* internodal cell was inserted into the open end. The ability of the cell to compress the gas within the capillary allows its turgor pressure to be measured directly. The first prototype of a leaf turgor pressure probe was developed by Zimmermann et al. in 1969 [54]. This consisted of a pressure screw connected to a silicon membrane in turn connected to a pressure transducer. This device allowed instantaneous data to be taken or recorded. Although this system was widely used and improved over time [55–57], it did not allow continuous, real-time data acquisition. In 2008, Zimmermann et al. developed leaf patch clamp pressure (LPCP) probes (Yara International, Oslo, Sweden), capable of continuous, non-destructive, real-time monitoring of leaf turgor pressure (Figure 1) [29].

The sensor was validated in *Tetrastigma vonierianum* plants grown in greenhouses [29]. The probe is composed of two metal magnetic pads. One of the pads incorporates a pressure-sensing chip. These magnets are strategically positioned on both the adaxial and abaxial sides of a leaf, ensuring that the pressure chip maintains close contact with the leaf surface. The distance between the magnets above and below the clamped leaf patch can be adjusted by regulating the separation between the two magnets, depending on the thickness and rigidity of the leaf. The sensors are connected by wire to a radio transmitter that sends the output directly to a gateway located in the field. After that, the output is transmitted to a server via a general packet radio service (GPRS) system. The data can be accessed via a cloud platform.



Figure 1. LPCP probe mounted in an olive leaf.

The sensor output (P_p) varies with the distance between the two magnets and is inversely proportional to the turgor pressure (P_c). For example, as the P_c decreases in response to daytime stomatal opening, the P_p gradually increases. Conversely, when stomata close at night, causing an increase in the P_c , the P_p gradually decreases [9,58]. Nevertheless, in olive (*Olea europaea* L.), it has been observed that, as water stress increases, P_p values tend to drop causing a semi-inversion of the curve under moderate stress situations, and a complete inversion at severe stress conditions [58–61]. Moreover, the output signal may vary with the tree height [29]. In addition, leaving the probe in the same leaf for too long could cause depigmentation of the sensor area due to a loss of chlorophyll, causing altered measurements as a result [26]. Specifically, data from the electrical output of the sensor were coupled with actual leaf turgor pressure data determined by the method developed by Zimmermann et al. in 1969 (described previously) [54]. A validation process was carried out over a wide range of turgor pressures (0–100 kPa), thus considering a full hydration status of the plant up to severe water stress. In the following years, LPCP sensors have been tested in various horticultural crops, such as in grapevine (*Vitis vinifera* L.) [62], grapefruit (*Citrus x paradisi* Macfad.) [62,63], nectarine (*Prunus persica* L.) [64,65], persimmon (*Dyospiros kaki* L.) [66,67], clementine (*Citrus clementina* Tanaka) [66], and olive [58–61,68–70]. In olive, they have been extensively tested with excellent results, indicating great reliability of the sensors for both ecophysiological studies and irrigation scheduling. Sghaier et al. [71] utilized these probes to study the effect of three irrigation levels on the water relations of young ‘Koroneiki’ and ‘Picholine’ olive trees, demonstrating the suitability of the sensors to monitor plant physiological and biological mechanisms [71]. In 2016, Padilla-Díaz et al. established an irrigation plan using such sensors to monitor the PWS in a hedgerow ‘Arbequina’ olive orchard. In detail, the authors found that the relation between the output trend and the tree water stress levels is robust for olive trees of different ages under a wide range

of growing conditions [60]. To identify actual water stress thresholds, recent studies have suggested monitoring other plant organs as well by combining the use of LPCP probes with other sensors and instruments. Rodríguez-Dominguez studied the sensitivity of olive leaf turgor to the air vapor pressure deficit (VPD), finding strong relationships. Moreover, the authors normalized their P_p data with the VPD values in order to predict the diurnal maximum stomatal conductance ($g_{s,max}$) measured with an open flow gas exchange system (IRGA Li-6400; LI-COR Biosciences, Lincoln, NE, USA) in olive trees grown in a hedgerow orchard. The sensors were proven to be highly reliable in predicting $g_{s,max}$. In nectarine, Scalisi et al. tested the combined use of LPCP probes and fruit gauges, demonstrating the suitability of a dual-organ sensing approach for the improved prediction of tree water status [64]. In 2020, Scalisi also confirmed the effectiveness of these two sensors when used together for detecting plant water stress in two olive cultivars ('Nocellara del Belice' and 'Olivo di Mandanici'). In the same trial, the authors also demonstrated the suitability of the probes to predict stomatal conductance and stem water potential [68].

Barriga et al. have developed a new expert system based on machine learning (ML) techniques together with an IoT infrastructure based on continuous measurements of leaf turgor pressure, providing very important information for irrigation scheduling [72]. The study shows that the ML models and the developed algorithm are valid for sweet orange (*Citrus sinensis* (L.) Osbeck cv. Navelina), while subsequent studies should test these models on other orange varieties and other citrus species, like lemon or tangerines (Barriga et al., 2022). Another model was proposed by Palomo et al. based on ML techniques to classify olive (*Olea europaea* L.) trees (cv. Arbequina) into three distinct levels of water stress by analyzing daily data trends [73].

2.1.2. Leaf Water Meter

A recent non-invasive leaf-mounted sensor developed and made commercially available to assess plant water status is the leaf water meter (LWM; Pastella Factory S.R.L.S., Verona, Italy). This optical sensor was developed in 2022 by Brunetti et al. [74] and is based on the photon attenuation during the passage of light at specific wavelengths (about 1450 nm) through the leaf, the signal intensity of which is related to the leaf water content. The LWM is composed of three plastic wires connected to a controller equipped with additional sensors (soil moisture sensor, temperature, relative humidity, and PPFD) and a LoRa module to transmit data via radio frequencies. The main sensor consists of a plastic clamp with a pair of LEDs and photodiodes inside, to be placed in the abaxial and adaxial parts of the leaf, respectively. The two pairs (LEDs and photodiodes) operate at two specific wavelengths, producing an electrical (analog) signal that correlates with the leaf water content. Specifically, one LED is set at 1450 nm (SWIR) and the other at 890 nm (NIR). The first is directly related to water status assessment [75,76], while the second is mainly linked to dry matter [74]. Also, in this case, the data are transmitted (through a LoRa module) to a gateway located in the field that sends the data directly to an internet server. The data are accessible in a cloud. The acquired data express the leaf dehydration level (DL). These need to be normalized by the feature scaling method (min-max normalization) to have comparable data between sensors.

This sensor was first tested by Brunetti et al. in 2022 in woody crops with different morphologies and biological characteristics (*Citrus limon* L., *Olea europaea* L., *Acer platanoides* L., and *Arbutus unedo* L.). A strong correlation was found between the DL and both the Ψ_{stem} and, especially, the leaf RWC ($R^2 = 0.73$ and $R^2 = 0.84$, respectively). The significance of estimating the RWC lies in the ability to bypass leaf osmotic regulation phenomena, providing more accurate data regarding the plant's actual hydration status [33]. Hence, the results of the first test demonstrated that the LWM can be a reliable and non-destructive alternative sensor for the continuous and real-time assessment of leaf water status in woody crops. Nevertheless, no other study employing the LWM has been conducted to date that confirms the sensor's reliability. Therefore, its official validation on other

economically significant fruit tree species (e.g., apple, pear, peach, grapevine, etc.) under various agro-environmental conditions is still pending.

2.1.3. Leaf Thickness Sensors

The relationship between leaf thickness and plant water status has been known for a long time. Basically, changes in leaf thickness are the result of water exchanges between the plant or the atmosphere and the leaf [77]. The leaf thickness undergoes changes not only due to oscillations in leaf water content, but also in response to various physiological and environmental mechanisms [78]. For instance, the leaf thickness exhibits diurnal-nocturnal cycles: in well-irrigated plants, the leaf thickness remains relatively constant during nighttime, decreasing throughout the day until reaching the minimum peak at solar noon [77,79]. Furthermore, leaf thickness shows a negative correlation with the VPD and light [80,81]. Thus, environmental factors influence leaf thickness changes by affecting the transpiration process [82,83].

The first studies were carried out in 1922 by Bachmann [84], followed by Meidner (1952) [77]. The latter was the first to use a gear micrometer to measure changes in leaf thickness continuously. He also observed a strong correlation between leaf thickness and leaf water content. In 1987, Búrquez used a spring-loaded gear-wheel micrometer in different herbaceous crops, finding strong correlations between leaf thickness and RWC ($R^2 = 0.96\text{--}0.99$) [81]. However, these instruments were found to be impractical and unable to make automatic and continuous measurements. In subsequent years other less bulky and more accurate devices were developed, mainly based on the principle of a differential transformer, i.e., linear variable displacement transducers (LVDTs) [85–87]. Seelig et al. designed an efficient irrigation scheduling method on cowpea using a miniaturized leaf thickness sensor consisting of electrical distance transducers [79]. Sharon and Bravdo conducted a comparison of irrigation scheduling methods, including continuous leaf thickness monitoring and four conventional drip irrigation regimes based on schedules and water depletion [87]. The results showed that the sensor-based drip irrigation treatment achieved the highest yield and exhibited the greatest water use efficiency for ‘Oroblanco’ grapefruit.

In 2017, Afzal et al. integrated leaf capacitance and leaf thickness measurements into a single sensor to investigate whether the combination of the two measurements can be used as an indicator of PWS [83]. In detail, the sensor consists of a clamp with two sensing units, one capable of measuring leaf thickness and the other capacitance. The thickness is measured by a pair of magnets, and based on their distance, measurements of leaf thickness (which depends on leaf turgor) can be obtained. A PCB is connected to the sensors via wires, and through a transmission module, it sends data to an internet-connected central unit. In summary, it is a kind of combination of LPCP probes and LMCS. The device was tested on tomato plants. From initial results, it was observed that changes in leaf thickness reflect the leaf transpiration rate, while capacitance is strongly related to the light period and photosynthesis. Thus, capacitance can be a reliable indirect measure of PWS through the water–photosynthesis relationship. Despite its reliability and simplicity, there are no studies on this sensor being applied in fruit crops. Indeed, variations in leaf thickness and capacitance may differ from one species to another and environmental variables may strongly influence sensor data. Hence, further studies are needed to validate the sensor. Currently, the sensor is not commercially available.

2.1.4. Leaf-Mounted Capacitance Sensor (LMCS)

In 2023, Talheimer developed the leaf-mounted capacitance sensor (LMCS) (Figure 2) [88]. This is a very low-cost sensor that is able to continuously measure a signal that follows the patterns of leaf transpiration and solar irradiance. The sensor is based on the approach of sensing leaf transpiration flow by forcing water vapor to condense in the leaf blade, whose temperature is below the atmospheric dew point [89]. The condensation process is driven by a declining temperature gradient, resulting from the decreasing temperature across the sunlit leaf and the underneath sensor plate. The sensor is based on a capacitive

principle and incorporates a photodiode as a light sensor. Simultaneously and continuously measuring incident light and leaf transpiration enables a qualitative assessment of the PWS. This estimation involves comparing the pattern of plant transpiration with the fluctuation in solar irradiance, which acts as its main driving force [90]. The sensor consists of a circular printed circuit board (PCB) and a photodiode. The circular PCB represents a capacitance sensor that can provide different outputs (in pF) depending on the vapor deposition in the lower leaf lamina. For this reason, the circular PCB has to be placed in contact with the lower leaf blade (Figure 2B). The sensors are then connected to a battery-powered Arduino-based microcontroller. Capacitance and irradiance data are transmitted via LoRaWan to an internet-connected gateway. Thus, the data can be accessed via a cloud. An additional strength of this device is its low cost due to its simple components. The use of the principle of capacitance to estimate leaf transpiration was studied by Afzal et al. in 2017 [91].

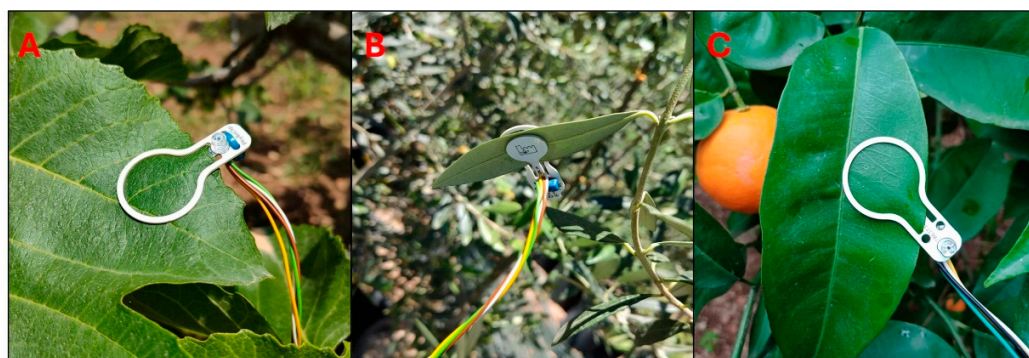


Figure 2. LMCS sensors mounted in fig (A), olive (B), and orange (C) leaves.

The sensor was first tested in 2023 in several perennial species: grapevine, persimmon, walnut (*Junglans regia* L.), olive, and apple (*Malus domestica* Borkh.). For instance, grapevine leaves revealed a signal indicating severe water stress under drought conditions, and a restoration of conditions (curve rise) after rainfall events and irrigation. Carella et al. (unpublished data) correlated the capacitance output of an LMCS with VPD data in fig (*Ficus carica* L.), finding a similar relationship to that between transpiration and the VPD which is already well-documented in the literature. Specifically, the relationship follows a hysteretic pattern due to the lag time of the stomatal response [92–94]. In detail, the capacitance increases more and more slowly as the VPD increases, until it reaches an asymptote where the capacitance becomes stable. In contrast, an inverse pattern was observed in the afternoon, in which, as the VPD decreases, the capacitance decreases more and more rapidly, until an asymptote is reached, indicating a transpiration stop. Clauser tested the LMC sensor in apple (cv Rosy Glow Pink Lady®), relating it to other technologies that measured soil moisture [95]. The results showed that this sensor allows for monitoring tree water status to define whether the lack of soil moisture is really a problem for the plant.

Since there are no other trials that use an LMCS, further validation studies of the sensor, e.g., by appropriate machine learning techniques, are needed to predict leaf transpiration and to evaluate the performance of the sensor under different climatic and physiological conditions of the tree. Furthermore, additional field testing will be essential to validate the sensor's long-term reliability and determine the most effective methods for integrating it into smart irrigation strategies across various crops and environmental conditions, with specific attention to crop performance and water use.

2.1.5. Continuous Thermal Sensing

Temperature is closely related to the PWS, since the physical principle behind changes in canopy temperature depends on the transpiration flow. Indeed, the closure of stomata caused by water deficit causes a reduction in leaf transpiration, consequently leading to an increase in leaf temperature [96]. Unfortunately, relying exclusively on leaf temperature

(T_c) may have several limitations due to the significant impact of environmental variables, including the wind speed, radiation, air humidity, and air temperature [97]. Therefore, it becomes imperative to normalize the data with other parameters (e.g., air temperature or a constantly heated thermocouple) or calculate vegetation indices to acquire thermal data that can be readily associated with plant physiological information, such as the crop water stress index (CWSI) [98,99]. Thermal sensors can be classified into contact and non-contact sensors. Among the contact sensors, the most widely used are thermal resistance sensors and the better-known thermocouples. The non-contact ones, on the other hand, are based on temperature measurement by infrared sensors or thermal imaging cameras [99].

A thermal resistance sensor is a temperature sensor consisting of a known resistance that varies with temperature, such as platinum resistance temperature measurement [99]. A thermal resistance sensor (LT-1T) was used to validate a system based on estimating plant water status using thermal images [100,101]. In 2012, Atherton et al. [102] developed a microsensor able to continuously and real-time monitor leaf temperature, in order to estimate leaf water content. The device is composed of a thin-film resistive heater and two thin-film thermocouple (TFTC) temperature sensors molded on a 10 μm -thick polyimide substrate. The sensor measures the leaf thermal resistance. The resistive heater generates a thermal gradient that changes in response to the overall thermal resistance of any sample in contact with the device. The resulting thermal gradient is measured as a temperature difference (ΔT) between the two TFTC sensors. The results achieved showed a strong positive linear correlation between the ΔT and leaf RWC. Despite its reliability and potential, the sensor has never been tested in horticultural crops or commercialized. Additional studies are necessary to establish specific thresholds for detecting water stress, to improve the sensitivity of the sensor and minimize its impact on plant health, possibly through design refinement or parameter adjustment. In addition, the effectiveness of the sensor under different environmental conditions needs to be thoroughly investigated to ensure reliable operation in various agricultural settings. In this regard, a thermocouple works as a transducer that converts thermal energy into electrical energy, and it is constructed by connecting wires made from different metals to create a junction. When the temperature at the junction changes, voltage is generated. The fundamental principle behind thermocouples is the Seebeck effect, which states that if dissimilar metals are joined at a point, they produce a small measurable voltage when the temperature at the connection point changes [103,104]. The magnitude of the voltage is determined by the extent of the temperature change and the characteristics of the metals. To date, thermocouples are used in validation operations for other techniques for estimating PWS by thermal sensing. For instance, Pou et al. utilized thermocouples for the validation of thermal indices for water status assessment in grapevine [105]. Costa et al. developed models to estimate water and heat fluxes in grapevine using leaf-mounted thermocouples and thermal imaging techniques [106].

In 2017, Dhillon et al. developed a continuous leaf monitoring system to assess plant water status by combining low-cost thermal infrared thermometers and environmental sensors [107]. The authors found a negative linear relationship between the ΔT ($T_{\text{leaf}} - T_{\text{air}}$) and stem water potential. Moreover, the combination of sensors provided enough data to accurately calculate the CWSI. The method was successfully tested in almond (*Prunus amygdalus* Batsch) and walnut (*Juglans regia* L.) [108]. Despite the demonstrated accuracy of the measurements, for a definitive validation of the system, studies on different crops and evaluation of the system performance under different conditions are needed to fully assess its potential as an irrigation scheduling tool.

2.1.6. Further New Sensors (Microsensors)

The emerging wearable electronics industry has shown promising results in various applications, although it is in its early stages in agriculture. The flexibility of wearable sensors allows their easy positioning close to specific plant organs and portions, facilitating

continuous and accurate monitoring. This capability helps in early plant stress detection and reduces plant productivity loss [109,110].

In addition to those already described, other interesting leaf-mounted sensors for PWS estimation have been developed in the past two years. In 2024, Peng et al. built a wearable and capacitive sensor for the real-time and precise monitoring of leaf water content. It was tested in golden pothos (*Epipremnum aureum* Lindl. and Andre) leaves [111]. The microsensor consisted of two wearable electrodes. The leaf must be placed between the two electrodes. Due to the excellent flexibility of the electrodes, the device can be used in a multitude of leaf types. The authors found that the leaf capacitance value is positively correlated with the leaf moisture content, and the results were similar to those found with conventional rigid electrodes [91,112]. Despite the results achieved and the high potential of the sensor, several problems remain to be solved. For example, attention needs to be paid to the leaf integrity when monitoring physiological information, which could be influenced by wearable electrodes. In addition, as the sensor has been tested for only a few days, it will be necessary to test it under open-field conditions and evaluate the timing of its measurement reliability. Im et al. built a flexible polyimide (PI)-based sensor, that is also based on the capacitance principle [113]. This microsensor proved useful for estimating the transpiration flux of tobacco plants grown in growth chamber conditions. Also in this case, although the sensor has demonstrated accuracy in its growth chamber measurements and is lightweight, it still requires testing under open-field conditions, particularly on fruit trees, to assess its consistency and durability.

2.2. Stem-Mounted Sensors

2.2.1. Stem Dendrometers

The plant water status can also be estimated by measuring diameter changes in different organs such as the stem, branches, and fruits [26]. Regarding the stem diameter variations (SDV), C3 plants follow a precise mechanism depending on the transpiration flow. In the early morning, as transpiration begins, the xylem water potential starts to decrease [114]. This tension extends from the foliage to the other organs of the plant, leading to the loss of water stored overnight [115]. Consequently, the plant responds to atmospheric water demand at a time when the root uptake is not fully active, acquiring water from other organs such as fruits, branches, and the trunk and causing daily fluctuations in their diameter [116,117]. In trees, the trunk's contribution to water transfer is significant [118]. Thus, a reduction in diameter occurs due to this transpiration water withdrawal from xylem and phloem vessels [119]. During the evening and night, the water potential is restored, and the trunk returns to its volume or increases, depending on the amount of carbohydrates gained during the day [120]. The fluctuation amplitude depends on the elastic properties of the tissues [117], the difference in osmotic pressure between the bark and xylem [121], the diffusive properties of water in the phloem [122], and the growth rate of the trunk [117].

From measuring changes in stem diameter, several SDV-derived indicators can be taken into account to assess PWS, e.g., the trend of maximum and minimum daily growth, daily growth, stem growth rate (SGR), and maximum daily shrinkage (MDS) [9,123]. The two last indicators are the most widely used [114].

The first prototype dendrometer (dendrograph) was built in 1883 by Böhmerle [124]. The use of automated dendrometers, on the other hand, has occurred since the second half of the 20th century [9,125,126]. Nowadays, the most commonly used dendrometers are optical types (infrared distance sensor [127]), electronic point dendrometers [128,129], and strain gauges with linear variable differential transformers (LVDTs). The majority of authors have used LVDT-type sensors, mainly because they are easy-to-use and low-cost [9].

Naor and Cohen utilized LVDT dendrometers to study the sensitivity and variability of the maximum daily shrinkage, midday stem water potential, and daily transpiration rate in response to withholding irrigation from field-grown drip-irrigated 'Golden delicious' apple trees [130]. The authors observed that both the MDS and Ψ_{stem} exhibit higher sensitivity to

variations in the soil water availability compared to the daily transpiration rate (determined using a 'Class A' evaporation pan). Moreover, the MDS was more responsive than the Ψ_{stem} to changes in the soil water availability. This may be explained by the non-linear relationship between the Ψ_{stem} and MDS [130,131]. However, they found that the MDS showed a higher variability than the Ψ_{stem} . In particular, the MDS's variability increased with the water stress. Therefore, the authors concluded that more measures than just the Ψ_{stem} and MDS need to be integrated. Additionally, establishing an irrigation scheduling threshold based on MDS measurements is likely to be more complex because thresholds may vary from one apple commercial plot to another due to changes in parameters influencing trunk bark thickness, such as the tree age and rootstock. More recently, Wheeler et al. utilized stem dendrometers to determine the tree water status of high-density apple orchards [132]. They aimed to enhance the precision of irrigation scheduling by correlating continuous data obtained from stem dendrometers with the Ψ_{stem} and atmospheric evaporative demand. On the other hand, in peach trees (*Prunus persica* L.), Conejero et al. showed that using dendrometers alone and calculating the MDS is sufficient for irrigation scheduling [133]. These results were confirmed by Mirás-Avalos et al. [134] and De la Rosa [135] in 2017 and 2016. In almond, on the other hand, the stem growth rate (SGR) was found to be more reliable than the MDS for assessing water status [136]. In pear (*Pyrus communis* L.), the MDS was found to be a good indicator of water stress, due to the quick response to environmental conditions [137]. On the contrary, Blanco and Kalcsits found that, despite the MDS detecting water stress earlier, it did not increase in the same proportion as the Ψ_{stem} when it was lower than -1.4 MPa [138]. In a table olive orchard, Corell et al. showed that both the TGR and MDS were found to be reliable indicators to detect mild water stress, even though they were less reliable than the Ψ_{stem} [139]. In cherry (*Prunus avium* L.), the MDS was less precise than the Ψ_{stem} but more sensitive and responsive to water stress, making it useful in situations where even a slight water deficit could impact the vegetative growth, fruit development, and yield [140]. In grapevine, the MDS and TGR were found to be unsuitable to predict water stress after veraison [141]. Finally, it can be stated that, while the measurement of the trunk diameter to assess the PWS can prove reliable depending on the crop, phenological stage, and water stress level and is easy to apply, it does not provide comprehensive information regarding the leaf and fruit water status [9,26].

2.2.2. Microtensiometers

The stem water potential (Ψ_{stem}) is considered one of the main indicators for assessing plant water status. However, as indicated previously, the most reliable method to measure the Ψ_{stem} has been the pressure chamber method, which is labor-intensive and time consuming. Fortunately, in recent years, devices that can measure the Ψ_{stem} continuously and in real-time are being developed. Recently, people at Cornell University together with the FloraPulse (FloraPulse Co., Davis, CA, USA, www.florapulse.com) company developed an electro-mechanical system-based microtensiometer which can be embedded in the trunk and is capable of measuring water potential continuously. This sensor was first described by Pagay et al. in 2014 [142]. In 2019, Black et al. published a detailed description of the sensor with its physical principle, also adding improvements [143]. The sensor is based on the tensiometer principle, i.e., an instrument able to monitor the water potential of an external matrix (xylem) by balancing an internal volume of water, where the hydrostatic pressure is considered the negative counterpart of the external water potential [144,145]. In brief, the microtensiometer combines two common sensing circuits: a strain gauge and a thermometer. The thermometer is made of a serpentine thin film platinum resistance (PRT), which changes its resistance with the temperature. The strain gauge consists of four polycrystalline silicon resistors (piezoresistors) in a Wheatstone bridge configuration placed on a diaphragm, and its resistances vary with the strain. Below the strain gauge, a 3 μm -deep cavity is etched with a diaphragm and a water reservoir [143]. Also in this case, data can be transmitted either via a wireless system or downloaded from a datalogger. The sensor is capable of continuously monitoring the trunk water potential (Ψ_{trunk}), thus providing

another tree water status indicator [142,146]. Although, in early studies, it was thought that the sensor directly measured the Ψ_{stem} , Pagay et al. showed that, in grapevine, there were differences between the Ψ_{stem} measured with the pressure chamber and the Ψ_{trunk} [144]. Specifically, the Ψ_{trunk} was generally higher than the Ψ_{stem} measured at the same time. The authors deduced that this difference is mainly due to hydraulic resistances between the trunk and leaves. Zucchini et al. also noticed this difference between the Ψ_{trunk} and Ψ_{stem} in olive trees [147]. In particular, they observed that, in 32 out of 33 measurements, the Ψ_{stem} data obtained using the pressure chamber were lower than the Ψ_{trunk} , with a maximum difference of 1.15 MPa. On the other hand, in almond [146] and nectarine [148], the Ψ_{trunk} and Ψ_{stem} were found to be quite similar. Due to such differences, new thresholds of water stress need to be established using Ψ_{trunk} .

The microtensiometer was first field tested on two grapevine cultivars, Shiraz and Cabernet Sauvignon [144]. The author characterized the seasonal and diurnal dynamics of the Ψ_{trunk} and compared these values with the Ψ_{stem} and Ψ_{leaf} measured with the pressure chamber. He found that the Ψ_{trunk} correlated better with the Ψ_{stem} than with the Ψ_{leaf} . Moreover, he showed that the relationship between the Ψ_{trunk} and Ψ_{stem} is stronger under low VPD than under high VPD conditions. In details, under high VPD conditions, the Ψ_{trunk} consistently declined below the Ψ_{stem} around mid-afternoon, followed by a recovery observed by early evening. The author concluded that the microtensiometer provided good measurement reliability and several studies will be needed to establish irrigation thresholds.

Blanco and Kalcsits tested the microtensiometer in pear by relating the Ψ_{trunk} and Ψ_{stem} measured with pressure chamber and found strong correlations, concluding that microtensiometers provide an accurate continuous method for measuring the water potential in trees throughout the growing season, even under diverse environmental conditions and variations in soil water content [149]. In 2023, Blanco and Kalcsits again published the results of 2 years of monitoring a pear orchard [138]. The authors found a strong correlation between the Ψ_{stem} and Ψ_{trunk} ($R^2 = 0.88$), and variations in trunk diameter (measured with a LVDT dendrometer) followed changes in the Ψ_{trunk} mainly at the beginning of the irrigation season. Once again, the sensor demonstrated high reliability for continuous PWS assessment. Kisekka et al. compared and evaluated data recorded on almond leaves with a Scholander chamber, microtensiometers, and osmotic cells for continuous measurement of the Ψ_{stem} [150]. The excellent results confirmed the potential of these sensors in facilitating irrigation scheduling.

Nieto et al. studied the relationship between the Ψ_{trunk} and fruit growth rate and managed to determine irrigation thresholds in apple trees [151]. In detail, through logistic regression analysis between the Ψ_{trunk} and fruit growth rate (in terms of fruit weight), the authors identified the critical value of approximately -0.97 MPa, which corresponded to the irrigation intervention threshold in that ecosystem. Satisfactory results regarding the suitability of microtensiometers to assess PWS were also obtained in nectarine [148] and almond [146,152] orchards.

Despite its reliability, the usefulness of the data, and its ease of installation, the sensor still needs to be validated at wider ranges of plant hydration given that so far it has been tested down to about -3.5 MPa (as also indicated on the FloraPulse website). Indeed, in species such as olive, especially in areas characterized by water scarcity, it is important to have a reliable sensor also at Ψ_{stem} values below -3.5 MPa [69,153]. Also, at least for strict determinations of tree water status, a 20–30-min time lag of the microtensiometer readings compared to actual Ψ_{stem} values has been observed, which must be taken into account, especially when daily curves are being studied. Additionally, there are still no studies where the microtensiometer has been employed for more than two consecutive years. Finally, the high cost of the sensor may represent a limiting factor for many growers and agricultural areas.

2.2.3. Sap Flow Sensors

The transpiration flow is closely dependent on the PWS, as the latter influences stomatal opening and thus gas exchange between the plant and the atmosphere. Nevertheless, in parallel with PWS, the transpiration (and thus sap flow) can be affected by environmental factors (VPD) [154]. The transpiration rates of whole trees can be assessed by sap flow methods that quantify the rate at which sap rises through the stems [155]. Such methods are collected on the dedicated working group web page of the International Society for Horticultural Science (ISHS) (<https://www.ishs.org/sap-flow/ishs-working-group-sap-flow-online-resources>, accessed on 12 May 2024), and recently Noun et al. published a review on plant-based methodologies and approaches for estimating the plant water status of horticulture crops in which there is an exhaustive update on methods for measuring sap flow [10]. In addition, there is SAPFLUXNET (<https://sapfluxnet.creaf.cat/>, accessed on 12 May 2024), a global database maintained by the Centre for Ecological Research and Forestry Applications (CREAF) (Barcelona, Spain), which aims to advance scientific understanding of the ecological factors that determine plant transpiration and drought responses worldwide [156]. One of the main advantages of sap flow sensors is that they are easily automated for continuous measurements [10].

Sap flow can be defined in terms of the sap flow rate (g or L h⁻¹ or equivalent) or sap flux density (sap flow rate per sapwood area) [157]. Flo et al. split the methods into four groups depending on their physical principle [157]: (1) dissipation [158,159], (2) pulse [88,160–166], (3) field [167], and (4) balance [38,168]. Such methods are briefly described in the following table (Table 1):

Table 1. A list of the main techniques for measuring sap flow, with brief descriptions.

Method		Brief Description	References
(1) Dissipation		It measures heat dissipation from a heated probe inserted in the sapwood compared to a non-heated reference probe	
Thermal dissipation	TD	The upper probe is constantly heated, and the measured temperature difference decreases with increasing sap flow density	[158]
Transient thermal dissipation	TTD	It works under transient conditions by introducing a relatively short heating and cooling cycle	[159]
(2) Pulse		It applies heat intermittently and monitor changes in sapwood temperature induced by thermal convection and conduction	
Compensation heat pulse	CHP	A heater probe is inserted into the xylem between two temperature sensors. By measuring the time, it takes for the heat pulse to travel via convection to the midpoint, the velocity of the pulse is determined	[160]
Heat ratio	HR	It employs a brief heat pulse to trace water movement, and by analyzing the heat ratio between two symmetrical temperature sensors, the magnitude and direction of water flow can be determined	[161]
Cohen's heat pulse	T-max	It uses a single temperature sensor located downstream of the heater probe. The sap flow rate is calculated from the time it takes the downstream temperature sensor to register the maximum temperature rise	[162]
Calibrated average gradient	CAG	Useful for calculating low sap velocities from sap flow records obtained with the standard CHP method, but the temperature differences between the readings of the two temperature probes are averaged (ΔT_a) over a certain period of time.	[163]
Sapflow+	SF+	It uses a four-needle sensor to measure heat velocity in the entire density range of natural sap flow and allows simultaneous estimation of stem water content	[164]

Table 1. Cont.

Method		Brief Description	References
Single probe heat pulse	SPHP	It uses a single-probe sensor based on the fundamental conduction–convection principles of heat transport in sapwood	[165]
Dual heat pulse	Dual	It combines two heat-pulse methods: The HR, effective for low and reverse flows, and CHP, suitable for moderate to high flows, within a single set of sensor probes	[166]
Ratio heat pulse	T _m Ratio	It uses the ratio of temperature maxima on downstream and side probes	[88]
(3) Field		It measures the shape variations of a continuous heat field within the sapwood by utilizing tangential and axial probes	
Heat field deformation	HFD	It uses a sensor composed of one needle-like heater inserted in the sapwood and three temperature sensors placed above, below and at the side of the heater	[167]
(4) Balance		It measures the energy balance through a heated wood section	
Stem heat balance	SHB	It involves employing a sensor with a flexible heater, typically several centimeters wide, encircling the stem and protected by layers of insulating and weather-resistant materials	[38]
Trunk heat balance	THB	It consists of three to five stainless steel metal plates inserted in parallel into the sapwood, spaced two centimeters apart, covering the entire sapwood depth. This configuration allows for the integration of sap flow across the sapwood.	[168]

Sap flow sensors based on the principle of thermal dissipation have been widely used in the literature [156]. Their popularity likely stems from their reliability, simplicity, and cost-effectiveness, as well as the ease of construction of handmade probes [169]. In 1985, Granier developed a thermal sensor consisting of two needle-shaped probes inserted radially into the sapwood [158]. One of these probes is heated at constant power, while the other serves as a temperature reference. In detail, a thermocouple (copper-constantan) is placed in the middle of the heating resistor, and an aluminum sheath covers the entire system to equalize the temperature. The second probe, positioned in the trunk below the previous one, contains an identical thermocouple mounted in opposition to that of the heating element. The system then permits measurement of the temperature difference (ΔT) between the two probes [170]. The author also found experimentally that the volumetric sap flow density (u , $\text{cm}^3 \text{cm}^{-2} \text{s}^{-1}$) is related to the temperature (T) by the following relationship (calibrated for different woody crops):

$$u = 0.119 \times K^{1.231} \quad (1)$$

In which:

$$K = \frac{\Delta T_{\max} - \Delta T}{\Delta T} \quad (2)$$

where ΔT_{\max} represents the maximum temperature value (when $u = 0$, i.e., during the night) and ΔT is the temperature difference between the two probes. In addition, the total sap flow (F , $\text{cm}^3 \text{s}^{-1}$) can be calculated from the sap flow density using the formula:

$$F = u \times A_{\text{sw}} \quad (3)$$

In which A_{sw} is the cross-sectional area of the sapwood (cm^2) [170].

The latter estimate (F) can be used for appropriate precision irrigation management since it is possible to estimate the actual volume of water transpired by the tree in the unit of time. The sensor was initially validated on forest species [158,170], but over the years it has been widely used in fruit crops. However, considering the high sensitivity of sap

flow to weather conditions, sap flow sensors often require calibration in the field [171] and, therefore, it is highly recommended to use them in conjunction with other sensors, such as LPCP probes and/or fruit gauges [9,25,26]. Fuchs et al. performed recalibration and comparison tests between TD and HFD methods [172]. The results showed that TD probes tend to underestimate the flux density by 23–45% with Granier's original calibration. The accuracy improves by performing species-specific recalibration. In contrast, HFD sensors overestimate flux by up to 11%. Under low and medium sap flow conditions, the HFD method underestimates the flux by 0.8%, thus demonstrating high accuracy. The authors concluded that both HFD and TDP sensors require new species-specific calibrations to improve their measurement accuracy. Furthermore, sap flow systems are currently not affordable for a significant portion of the agricultural community.

Despite these issues, sap flow has been used as an indicator for water stress in several cases. On apple trees, Nadezhdina used a sap flow index estimated by the heat pulse velocity (HPV) method that proved sensitive to water stress, with a strong correlation with the pre-dawn Ψ_{leaf} ($R^2 = 0.96$) [167]. Hernandez-Santana et al. [173] correlated sap flow data with the gas exchange in olive trees. They found that stomatal conductance (g_s) and net photosynthesis (A_n) can be readily estimated from sap flow. Ferrara et al. used sap flow meters with the thermal dissipation method to evaluate the influence of the water deficit on the water use efficiency and water productivity in olive trees (cv. Arbosana) cultivated in an adult super-high-density orchard [174]. In orange (*Citrus sinensis* Osbeck), Cohen's heat pulse (T_{max}) sap flow was successfully used to identify water stress conditions [175]. In cherry, the joint use of sap flow sensors and dendrometers (MDS) represented a suitable system for irrigation scheduling [176]. Marino et al. included continuous TD probes in a multiple plant-based sensing system to detect mild water stress in olive [58]. The authors concluded that sap flow probes are not as useful as LPCPs and fruit gauges for detecting water stress in olive because they are strongly influenced by VPD. However, they can provide a useful quantitative indication of transpired water.

2.2.4. Thermocouple Psychrometer

An additional non-invasive method to monitor the water status of a plant through water potential is using thermocouple psychrometers. These instruments allow for determining the Ψ_{leaf} or Ψ_{stem} . The principle is based on the Seebeck effect, which consists of a complete electrical circuit formed by two dissimilar metals forming a thermocouple. If the measuring and reference junctions of the circuit are at different temperatures, a voltage difference, which depends on the temperature difference between the junctions, will be generated by a flowing current [98]. In thermocouple psychrometry, the relative humidity of the air around the sensing junction is crucial because it affects the temperature difference between the wet sensing junction and the dry reference junction [177]. To directly calculate the water potential from the measurements, the instrument needs to be empirically calibrated using solutions of known water potential [178]. This method started to be used around the 50s. Initially, psychrometry was only used in the laboratory because it required accurate temperature control. Over time, advancements in new projects and electronic instrumentation have provided the capability to perform on-site measurements quickly and non-destructively. There are currently three types of psychrometers: non-equilibrium, isopiestic, and dew point psychrometers [179]. Nowadays, the most used psychrometer is the PSY1 Stem Psychrometer built by Dixon and Tyree and currently produced by ICT International (Armidale, NSW, Australia) [180]. The PSY1 Stem Psychrometer consists of two soldered chromel-constantan thermocouples connected in series inside a chrome-plated brass chamber that forms a large thermal insulating mass. Inside the chamber, one thermocouple is in contact with the stem sample and the other simultaneously measures the chamber air temperature and, after a Peltier cooling pulse, the wet bulb depression. A third copper-constantan soldered thermocouple is located inside the sample chamber body to measure the temperature of the instrument for temperature compensation purposes. The use of the PSY1 Stem Psychrometer has proven to be reliable for monitoring the water

potential, after validation with other techniques, including the Scholander pressure chamber [181,182]. Kokkotos et al. used the PSY1 Stem Psychrometer to evaluate the variation in water potential in response to alternate fruit bearing [183]. In this study, the instrument was calibrated with a NaCl solution, and the water potential data were acquired every 30 min. In another study carried out in olive [184], water potential measurements were taken every 20 min, and the purpose was to evaluate how the hydraulic conductance changes in plants under water deficit. The PSY1 Stem Psychrometer was also used on grapevine to evaluate the plant response to a 6-week drought experiment [185]. In conclusion, the use of the PSY1 Stem Psychrometer has proved to be a very valid method for the continuous measurement of stem water potential [186]. Despite the sensor's reliability, the main disadvantages can be related to the need for calibration with standard solutions, difficult installation, and high cost [186].

2.2.5. TreeTalker[®]

The TreeTalker[®] is a continuous real-time system that was developed by Valentini et al. (Figure 3) to measure water transport in trees, radial trunk growth, spectral characteristics of leaves, and microclimatic parameters using artificial intelligence [127,187]. The instrument consists of a microcontroller with an ATmega 328 processor chip connected with different sensors designed for the measurement of plant physiological variables. The TreeTalker[®] includes a reference and a heated probe (Murata Electronics, Nagaokakyo, Kyoto, Japan) to measure the sap flow rate through the heat pulse method; a capacitive sensor to measure trunk moisture content; a 12-spectral-band spectrometer (AS7262 for visible and AS7263 for near infrared band—AMS, Premstaetten, Austria) centered at the wavelengths of 450, 500, 550, 570, 600, 610, 650, 680, 730, 760, 810, and 860 nm to measure the multispectral signature of light transmitted through the canopy; a MMA8451Q thermohygrometer (Silicon labs, Austin, TX, USA) to measure air temperature and relative humidity; an infrared distance sensor (SHARP, Osaka, Japan) to measure tree trunk radial growth; a Si7006 accelerometer (NXP/Freescale, Austin, TX, USA) to measure accelerations along a 3D coordinate system used to detect tree movements. The TreeTalker[®] has mainly been used in forestry but could potentially be used in fruit trees [188–190]. This device could be valuable for assessing both plant water status and consumption. Specifically, integrated sap flow probes can provide data on transpired water, while the infrared resistance sensor, capacitive trunk moisture sensor, and spectroradiometer can offer a good indication of the PWS. Such comprehensive information can be of great advantage for irrigation management. On the contrary, it requires a validation with PWS main references (RWC , Ψ_{stem}). To date, no experimental trials with TreeTalker[®] on assessing the plant water status and consumption and irrigation management of fruit trees have been conducted.



Figure 3. TreeTalker[®] mounted on an olive trunk.

2.3. Fruit-Mounted Sensors

Fruit Gauges

Fruit growth parameters can be a reliable indicator of PWS [191]. The total volume of the fruit is determined by the balance of water inflow and outflow through the phloem and xylem, along with atmospheric exchanges that occur through the exocarp [26]. Such water flows into and out of the fruit are determined from the water potential gradient differences between the plant and the fruit [191,192]. Similar to what happens in the trunk, water exchanges cause diametric fluctuations during the day. Furthermore, due to the composition of fruit tissues (relatively high water content compared to wood tissues), they exhibit greater sensitivity in diametric variation to changes in water potential gradients compared to the trunk. This increased sensitivity allows for timely measurements, which are useful in preventing adverse effects on fruit growth and final yields. Daily diametric fluctuations are due to the imbalance between the inflow and outflow. Indeed, during the midday hours, the fruit transpiration rate is higher than the xylem inflow (outflow > inflow), causing fruit shrinkage [193]. During the evening and night, water potential is restored, and the fruit returns to its original volume or expands thanks to the accumulation of carbohydrates during the day [193–195].

Since the second half of the 1900s, several studies have reported the use of devices to monitor fruit diameter [196–200]. Most of the sensors developed are LVDTs (strain gauges) connected to a plunger that makes direct contact with the peel, usually mounted in a metal frame [199]. The first rudimentary LVDT device for the continuous monitoring of fruit diameter was designed by Tukey in 1964 [196]. In 1984, Higgs and Jones devised an accurate system for the continuous measuring of fruit diametric fluctuations [197]. In 1998, Link improved the sensor by making it more flexible and suitable for greater thickness ranges [200]. Despite the accuracy and reliability of these sensors, they were relatively expensive and, considering the number of sensors required to be used in the field, non-sustainable for a farm [26]. In 2007, Morandi et al. constructed a low-cost sensor consisting of a linear potentiometer connected to a plunger that must be kept in contact with the peel and a stainless-steel frame (Figure 4) [199]. The gauge is adjustable and can be used with fruits of various sizes, from olive [68] to mango (*Mangifera indica* L.) [193]. To date, it is the most widely used type of fruit gauge in studies of fruit growth dynamics in response to external factors, including changes in PWS [65,69,201–203]. In 2016, Thalheimer built a fruit diameter monitoring sensor with low-cost optoelectronic components and with a flexible two-color tape for movement detection by the optoelectronic sensor [198]. However, while this sensor may prove useful for monitoring the active growth of the fruit, it does not seem suitable for assessing PWS because it is only able to detect fruit enlargements and it does not react to shrinkage. The latest sensor built for monitoring fruit growth was presented by Peppi et al. in 2023 [204]. It is part of a low-cost multi-channel sensor-node architecture capable of transmitting data with a low-power LoRa transmission system. The sensor structure consists of two solid arms bound together at one end with a bolt. The plier is held in place by a spring, while a reference voltage-supplied potentiometer is located within the fulcrum of the plier and rigidly connected to one of the two arms of the clamp. This seems to be a more stable sensor on the fruit and more suitable for IoT systems. However, it still needs to be validated in fruit crops.



Figure 4. LVDT fruit gauges mounted in loquat (A), orange (B), mango (C), olive (D), and peach (E) fruit.

Fruit gauges have been abundantly used to understand the physiological dynamics of fruit water exchanges, i.e., to study the relative contribution of xylem, phloem, and transpiration flows to fruit growth and understand the water relationships between a fruit, plant, and environment at different fruit development stages. These mechanisms were studied in peach [194], apricot (*Prunus armeniaca* L.) [205], kiwifruit (*Actinidia deliciosa* Chev.) [206], sweet cherry [207], and pear [208]. Carella et al. used fruit gauges to test the effect of the vapor pressure deficit (VPD) on the fruit relative growth rate (RGR), by comparing data of peach, mango, loquat (*Eriobotrya japonica* Lindl.), olive, and orange [209].

Several studies have investigated the suitability of the continuous monitoring of fruit growth to promptly detect when the fruit starts to be affected by water deficit in order to establish the moment to apply irrigation water. Boini et al. [210] monitored fruit growth to detect the onset of water stress in 'Imperial Gala' apples by correlating various growth parameters (fruit net daily growth, midday AGR, maximum AGR, minimum AGR, and fruit daily shrinkage) with the Ψ_{stem} . The results showed that the fruit daily growth rate (g day^{-1}) is the index that better correlates with the Ψ_{stem} , thus having the potential to be used as a reference in apple irrigation scheduling. In addition, the authors were able to define the threshold indicating the onset of moderate water stress in terms of the fruit daily growth rate (from 1.2 to 1.3 g day^{-1}). Khosravi et al. carried out a three-year study using fruit gauges to assess abnormalities in the fruit growth of 'Frantoio' olive trees due to several factors including tree water status. The purpose of the study was also to find the best way to analyze data with different statistical models [211]. Marino et al. used fruit gauges in conjunction with sap flow probes and leaf turgor pressure sensors (LPCP probes) [58]. The authors showed that the joint use of these three sensors can provide a comprehensive indication of olive trees' water status. For instance, the two olive cultivars studied showed different response behaviors to a water deficit: one manifested it in pronounced changes in its leaf turgor and fruit RGR, and the other significantly reduced its sap flow and reached very low values of leaf turgor pressure. In nectarine, Scalisi et al. demonstrated the suitability of a dual-organ sensing approach by using fruit gauges with LPCP probes to determine irrigation timing by assessing which organ and sensor exhibited the strongest correlation with the Ψ_{stem} [64]. Ultimately, it was found that a combination of both approaches proved most effective in determining irrigation timing. In 2020, Scalisi et al. replicated the experiment with olive trees and similarly concluded that a combination of leaf and fruit sensing proved most effective in determining irrigation timing [68].

Although monitoring the fruit diameter may be important to identify when fruits are adversely affected by water deficit (fruit is the strongest sink organ), these data alone may not be enough for a complete analysis, as its growth dynamics may be influenced by other factors like the crop load and mainly phenological stage [64]. In most stone fruits, water exchanges between the fruit and the plant or the atmosphere are at their lowest during pit hardening, while transpiration rate peaks during cell enlargement [212]. Having information from multiple organs simultaneously, such as the leaves and xylem, can be valuable for assessing the physiological behavior of the entire plant system across the stages of fruit development. Therefore, it would be necessary to use this sensor in combination with others, for example, sap flow and LPCP sensors, as previously shown.

3. Remote Sensing

Investigating the spatial and temporal variability in the field is one of the primary goals of precision irrigation. Ground-based measurements, although reliable, continuous in time, and accurate, provide a spot indication of the whole-field water status. Remote sensing techniques, although generally unable to monitor variability over time, are meant to overcome this spatial limitation of proximal measurements [45,213,214]. Remote sensors are capable of acquiring images containing information of different types and covering a wide area. In order to understand what type of sensor to use, one must be clear about the variable to be analyzed. Generally, remote sensors that are capable of measuring data reflected or transmitted by crops are used. This is because different components of the

canopy structure are capable of reflecting energy at different wavelengths depending on the molecules in the tissues. The spectral bands used in precision farming include ultraviolet (UV; 300–400 nm), visible (VIS; 400–700 nm), near infrared (NIR; 700–1400 nm), shortwave infrared (SWIR; 1400–3000 nm), and thermal infrared (TIR; 3000–25,000 nm) [46,215]. These spectral bands allow the calculation of vegetation indices (VI) that are useful in assessing plant physiological parameters, e.g., the normalized difference vegetation index (NDVI), crop water stress index (CWSI), normalized difference red edge index (NDRE), normalized difference water index (NDWI), etc. In this regard, remote sensors include optical cameras that are distinguished by various factors such as the type of operation to carry out, type of acquisition, and number of spectral bands [46]. In precision irrigation, thermal, multispectral, and hyperspectral sensors can provide accurate PWS information [6]. The main platforms used in remote sensing are satellites and unmanned aircraft systems (UAS, drones). Generally, satellites can provide a large amount of information since they can cover huge areas, but with a relatively low resolution [216]. Drones, on the other hand, manage to cope with the resolution problem since they can fly at closer distances (40–120 m above the ground) [217–220]. Nevertheless, with the growing prevalence of free satellite data sources such as MODIS, Landsat, Sentinel, and Gaofen, commercial satellite imagery resolutions continue to improve both spatially (WorldView) and temporally (Planet). This improvement is attributed to cost reductions in small satellite systems [221,222].

The following paragraphs briefly describe the main remote sensing techniques for assessing the field water status (FWS) in woody fruit crops by using thermal, multispectral, and hyperspectral sensors.

3.1. Thermal Sensing

Plant temperature has been a longstanding indicator of water availability [96]. In the last three decades, thermal infrared (TIR) cameras have proven to be effective tools for estimating leaf and canopy temperature (T_c), which has been recognized as a rapid, reliable, and non-destructive indicator of transpiration and PWS [223,224]. Plants tend to regulate their temperature by transpiring through the stomata, thereby balancing the energy fluxes within and outside the canopy [6,225]. When the plant undergoes stress, the transpiration rate decreases, leading to an increase in the T_c . This increase in the T_c may serve as an indicator for detecting plant water stress [46,225]. However, the T_c alone may not be sufficient, as it is influenced by various factors, mainly the air temperature (T_{air}). Several authors have often decided to normalize the canopy temperature with the air temperature ($T_c - T_{air}$) before correlating it with the main indicators of PWS (Ψ_{stem} , RWC, g_s , etc. . .) [66,226,227]. In 1981, Jackson et al. [96] developed the crop water stress index (CWSI), derived from the energy balance equation. In detail, the complete formula for CWSI is the following [98]:

$$CWSI = \frac{(T_c - T_{air}) - (T_c - T_{air})_{LL}}{(T_c - T_{air})_{UL} - (T_c - T_{air})_{LL}} \quad (4)$$

where $(T_c - T_{air})_{LL}$ is the lower limit of the difference between T_c and T_{air} , corresponding to a fully transpiring canopy. $(T_c - T_{air})_{UL}$ is the upper limit, corresponding to a non-transpiring canopy. $(T_c - T_{air})_{LL}$ is also defined as non-water stress baseline (NWSB), established through the relationship between $T_c - T_{air}$ and VPD; whereas $(T_c - T_{air})_{UL}$ corresponds to the relationship between the $T_c - T_{air}$ and VPD of a non-transpiring canopy. Conventionally, the $(T_c - T_{air})_{UL}$ is obtained from the intercept of the equation used to calculate the NWSB corrected for air temperature, according to the methodology proposed by Idso et al. in 1981 [98,228]. In 1999, Jones simplified the equation as follows [229]:

$$CWSI = \frac{T_c - T_{wet}}{T_{dry} - T_{wet}} \quad (5)$$

In which T_c is the actual canopy temperature obtained by thermal photo, and T_{dry} and T_{wet} are the references representing the non-transpiring leaf (or canopy) temperature and a fully transpiring leaf (or canopy) temperature, respectively. The CWSI ranges from 0 (fully hydrated plant) to 1 (fully stressed plant). One of the most debated issues concerns the methodology to establish T_{dry} and T_{wet} references. To date, several methods have been studied. One may involve a theoretical (or analytical) approach, determining the CWSI and references via the balance equation at the canopy surface. However, this method requires the use of several environmental parameters (for more details see Jackson et al. [230] and Agam et al. [231]). An alternative approach involves the use of a wet artificial reference surface (WARS) [232,233] as T_{wet} , while T_{dry} can be estimated empirically as $T_{air} + 5\text{ }^\circ\text{C}$ [234]. Nevertheless, the accuracy of this method could be significantly affected by the material of the WARS, which should have similar leaf emissivity [6,235]. Apolo-Apolo et al. built paper-based hemispheric surfaces that were placed in a 3D-printed plastic structure that continuously allows water storage [236]. Another common approach involves using leaves sprayed with water and detergent 30 s before measuring the leaf temperature as wet references. For the dry reference, the leaf is covered with petroleum jelly at least 30 min before the measurement to artificially close the stomata and inhibit transpiration [225]. Finally, a frequently used approach in recent studies involves extrapolating the temperature of the pure canopy from the entire thermal image through image analysis, aiming to obtain the temperature distribution histogram of the pure canopy. T_{wet} corresponded to the average temperature of the 0.5% values on the left side of the histogram, whereas T_{dry} to the average temperature of the 0.5% values on the right side [237–241]. The latter approach has proven reliable in different species such as nectarines [237], grapevine [242], plums (*Prunus domestica* L.) [243], and olive [241].

Image analysis is necessary to extract temperature values. The main methods for canopy extraction consist of selecting a region of interest (ROI), temperature threshold, and binary mask [244]. A ROI containing a single leaf or an area of leaves is identified in the thermal image either through manual or automatic delineation of an area mainly covered by leaves within the central portion of the thermal image [105]. ROI selection is rarely used for canopy segmentation in thermal imaging obtained by UAVs. This is largely due to the presence of significant ground background pixels in UAV-obtained thermal images, which makes it difficult to accurately isolate the canopy pixels. Temperature thresholding consists of distinguishing the soil and canopy pixels using a bimodal histogram showing two temperature peaks attributed to the soil and canopy [245]. Thus, temperature thresholding can be easily determined from the temperature frequency histogram of thermal imaging. Although most pure canopy pixels can be extracted, the temperature threshold has shown a lack of suitability for distinguishing canopies under severe water stress, because the T_c is higher than that of well-watered canopies and is likely to be improperly discarded as soil pixels [244]. This could lead to subsequent errors in the calculation of the mean canopy temperature and CWSI. Finally, for the binary mask technique, it is necessary to capture thermal and RGB images simultaneously. The binary mask is created by interactively determining the threshold values for the color components in the visible (RGB) images. The visible images are then processed to segment the canopy pixels according to color characteristics [246]. Afterwards, the segmented RGB image and the thermal image are perfectly overlaid to determine the temperature of the selected areas. Great care must be taken at this stage since a slight misalignment of the images will cause the soil background to be included in the thermal image, leading to errors in the calculation of the average canopy temperature (a problem that can be solved by a temperature thresholding operation).

In practice, CWSI from remote sensing has proved useful for estimating PWS in terms of both water potential (Ψ_{stem} and Ψ_{leaf}) and gas exchange (g_s) in woody fruit crops. Strong correlations have been shown in multiple crops, such as grapevine [105,238,247], olive [231,248–250], almond [251], plum [243], peach [237,245,252], apple [253], cherry [223], pear [227], and citrus [228,254,255], among others. In 2023, Mortazavi et al. developed a predictive model for determining the Ψ_{stem} in almond and pistachio using vegetation

indices obtained from aerial images through a machine learning approach [256]. Employing the random forest (RF) algorithm, which demonstrated higher accuracy (88% for pistachio, 89% for almond), they found that the CWSI played a more significant role in predicting the Ψ_{stem} in both crops.

Thermal imaging techniques can be applied with images from both unmanned aerial vehicles (UAVs) and satellites. Although thermal satellite imagery is mainly used to study climate change, due to the ease of access to low-resolution imagery, Landsat and Sentinel-2 have been frequently used in agriculture for CWSI calculation [257]. Jamshidi et al. [254] used both Landsat and Sentinel-2 data to assess the CWSI in citrus. The authors found strong correlations by comparing the CWSI calculated from satellite data and in situ CWSI obtained from UAV thermal imagery.

In summary, remote thermal sensing has proven to be a reliable method on from medium to large scales for assessing the water status of fruit trees. However, despite the strong and significant relationships between thermal indices and direct ground-based measurements, there are varying ranges of CWSI values, depending primarily on the methodology applied for calculating the different indices. Furthermore, it would be beneficial to develop models not only for individual species but also for different cultivars.

3.2. Multispectral Sensing

Reflectance data in the different bands can provide direct or indirect indications of PWS. The reflectance spectrum of water can be identified in the infrared region as there are overtone bands of OH bonds at about 760, 970, 1450, and 1940 nm (regions of the NIR and SWIR, respectively) [258,259]. Multispectral cameras are sensors that can commonly provide data in five or six spectral regions, usually included in the VIS, rededge, and NIR bands. Since multispectral cameras mounted in drones or satellites generally do not go beyond NIR, crop water status is often assessed by indices that provide an indirect estimate [260]. Chlorophyll or nitrogen content may prove useful indirect indicators of PWS. Therefore, indices have been developed that are calculated in the reflectance band of these molecules, i.e., in the VIS, rededge, and NIR regions [221,261]. The index that has been most widely used in fruit crops is the NDVI, calculated by considering the rededge and NIR reflectance [262]:

$$\text{NDVI} = \frac{\text{NIR} - \text{RED}}{\text{NIR} + \text{RED}} \quad (6)$$

When biotic or abiotic stress phenomena begin to occur, the reflectance of the NIR tends to decrease. In contrast, the reflectance of the RED increases. NDVI values range from -1 to $+1$. Negative values refer to soil properties, and positive to vegetation [263]. Numerous works have investigated the use of the NDVI to assess PWS. For instance, Ballester et al. [264] examined the effectiveness of multiple xanthophyll, chlorophyll, and structure-sensitive spectral indices from UAVs for identifying water stress within a commercial orchard that included five different species (apricot, almond, peach, orange, and lemon). The authors showed that the NDVI and photochemical reflectance index (PRI; a further VI calculated in the VIS region) were the indices that best correlated with the Ψ_{stem} ($R^2 = 0.61$ and 0.65 , respectively), whereas, for analyzing within single species, peach and ‘Garrigue’ almond were found to be the most suitable species for the prediction of both the Ψ_{stem} and g_s from NDVI data ($R^2 = 0.72$ and 0.74 for Ψ_{stem} and $R^2 = 0.75$ and 0.71 for g_s , respectively). In olive, Caruso et al. [265] demonstrated that the NDVI can be a reliable indicator of tree water stress. In grapevine, several works confirm that the NDVI can be a good indicator of PWS [266–269]. Other vegetation indices commonly used for PWS assessment, and which have been shown to be reliable, are the green normalized difference vegetation index (GNDVI), modified soil adjusted vegetation index (MSAVI), optimized soil adjusted vegetation index (OSAVI), green index (GI), normalized difference rededge index (NDRE), enhanced vegetation index (EVI), simple ratio index (SR), and water index (WI) [6,268,270–273]. Zúñiga Espinoza successfully used the green normalized difference vegetation index (GNDVI; a further VI calculated as the ratio between

the difference of NIR and Green bands and the sum of NIR and Green bands) for estimating the g_s in grapevine [261]. Stagakis found strong relationships between the PRI and Ψ_{stem} in orange [274]. In 2023, Fasiolo et al. introduced a novel method to assess the effects of different water regimes on the water potential, vegetation indices, and canopy geometric data in grapevine [275]. This approach combined geometric measurements gathered by a mobile robot with multispectral data obtained from a UAV, as well as traditional measurements like Ψ_{stem} and Ψ_{pd} (pre-dawn stem water potential). In detail, 60 vegetation indices were accurately calculated using the projected area of the vineyard point cloud as a mask. Among them, three vegetation indices were identified that correlated best with the Ψ_{stem} : the green difference vegetation index (GDVI; $R^2 = 0.90$), perpendicular vegetation index (PVI; $R^2 = 0.90$), and triangular greenness index (TGI; $R^2 = 0.87$). In addition, they observed that the canopy volume and area projected onto the ground were affected by the water status, as were measurements of the Ψ_{stem} and Ψ_{pd} . Their scientific contribution involved integrating multispectral data from UAVs with ground-based data from a robot, enabling the extraction of spectral information exclusively from plants while excluding non-canopy surfaces.

Also in 2023, Longo-Minnolo et al. developed a new combined approach based on the use of multispectral imagery from UAVs and statistical models to determine the water status of an orange orchard (cv. Tarocco Sciara) during different phenological stages, compared with the traditional Ψ_{stem} [276]. The results first indicate that significant correlations with the Ψ_{stem} were found for 9 of the 14 calculated vegetation indices: atmospherically resistant vegetation index (ARVI), EVI, MSAVI, NDRE, NDVI, OSAVI, renormalized difference vegetation index (RDVI), soil adjusted vegetation index (SAVI), and SR. Second, the use of statistical methods such as stepwise linear regression and principal component regression (PCR) with all bands and vegetation indices allows for more reliable Ψ_{stem} estimates. Both methods have comparable performances, with PCR showing slightly lower errors.

Satellite multispectral imaging provides different information with respect to drones. Satellites can provide images at a wider multispectral range. Sentinel-2 [277,278] and Landsat 8 [279], for example, are capable of obtaining information on the spectral bands of VIS, NIR, SWIR, and thermal infrared (TIR) [6]. Other satellites used for the water status of fruit crops are Landsat 7 [280], WorldView-2 [281,282], and MODIS [283]. In pear, Van Beek [281] successfully estimated the Ψ_{stem} through WorldView-2 multispectral imagery. In recent years, the Planet [284] platform has been developed, which uses a wide network of satellites (including PlanetScope, SkySat and RapidEye, Landsat 8, and Sentinel-2) to collect images and data from around the world. These satellites constantly capture information about the Earth's surface, giving users access to recent and historical images [285]. For example, Helman et al. used planet satellite images to monitor grapevine Ψ_{stem} [285]. In olive, Garofalo et al. [286] developed a machine learning algorithm to predict the Ψ_{stem} using Planet.

Since the spectral bands of water are the NIR and SWIR bands, with the use of satellites, indices can be calculated for direct estimation of PWS, such as the moisture stress index (MSI) [283] and the better-known normalized difference water index (NDWI) [287]. For instance, Rodríguez-Fernández found strong relationships between the Ψ_{stem} and NDWI ($R^2 = 0.67$) in grapevine [288]. Also in olive, the NDWI proved to be a reliable predictor of water potential [270].

Multispectral methods may prove useful for PWS assessment, albeit often indirectly (especially with sensors lacking the SWIR band). Moreover, it could be argued that handling this extensive amount of data and conducting image analysis requires specialized skills. Knowledge of GIS-based software for geographic data visualization, management, and analysis is crucial. Furthermore, the acquisition and management of these tools can be expensive, particularly when working with high-resolution imagery. This limitation may restrict access to such technologies for certain growers. Environmental conditions could also significantly affect the measurements. The reflection and refraction of sunlight on the Earth's surface can vary depending on environmental conditions, such as the presence of

fog, clouds, atmospheric dust, or humidity. These phenomena can affect the quantity and quality of the reflected light recorded by multispectral sensors, compromising the accuracy of the measurements [6]. Nevertheless, optimistic future prospects for multispectral remote sensing in PWS monitoring exist. The growing accessibility of this system, refinement of vegetation indices, and advancements in artificial intelligence may lead to the development of new models and ready-to-use systems for efficient irrigation management.

3.3. Hyperspectral

In recent years a rapid advancement in spectroscopic and imaging technologies has occurred. In this regard, hyperspectral remote sensing imaging (HRS) has emerged as an efficient nondestructive technique to monitor several plant physiological parameters [289,290]. Multispectral imaging involves capturing spectral signals in specific bands, covering a wide spectral range from tens to hundreds of nanometers. Hyperspectral imaging, on the other hand, captures spectral signals in a sequence of continuous channels with a narrow spectral bandwidth, usually less than 10 nm. This capability allows hyperspectral imaging to capture detailed spectral features of targets that might be overlooked by multispectral imaging [291,292]. Besides cameras, spectrometers are also used in HRS. A spectrometer analyzes the spectral signatures of ground features in the sensor's field of view by examining the spectral characteristics of light radiation and separating the incoming energy into various wavelengths. Unlike optical, multispectral, and hyperspectral cameras that capture multiple bands of the electromagnetic spectrum and offer continuous gridded pixel area coverage, a spectrometer provides coverage in single pixel footprints determined by its field of view. Nevertheless, its high spectral resolution makes it a viable alternative to multispectral sensors [293]. Both hyperspectral cameras and spectrometers are mounted on UAVs during remote sensing measurements. In addition, hyperspectral sensors are also mounted on some satellites. However, few studies have been carried out with satellite remote sensing. Moreover, compared to the large number of satellite-mounted multispectral sensors, there are fewer with hyperspectral sensors. These include EO-1 Hyperion (the most widely used in agriculture), Tian-Gong-1, PRISMA, and PROBA-CHRIS [235,292]. For future perspective, the European Space Agency (ESA) is developing the Copernicus Hyperspectral Imaging Mission for the Environment (CHIME). This will carry a unique infrared spectrometer in the visible and shortwave bands to provide routine hyperspectral observations to support new and improved services for the sustainable management of agriculture and biodiversity, as well as the characterization of soil properties. The mission will complement Copernicus Sentinel-2 for applications such as land cover mapping ([https://www.esa.int/ESA_Multimedia/Missions/CHIME/\(result_type\)/images](https://www.esa.int/ESA_Multimedia/Missions/CHIME/(result_type)/images), accessed on 12 May 2024) [294].

Various vegetation indices based mainly on NIR and SWIR bands (950–970, 1150–1260, 1450, 1950, and 2250 nm) can be determined from the hyperspectral sensors, such as the NDWI, water index (WI), and water band index (WBI), among others [6,295,296]. Specifically, the NDWI is calculated as the ratio between the difference in reflectance at approximately 860 nm and the reflectance at approximately 1240 nm bands, divided by their sum. Meanwhile, the WI is determined by the ratio of reflectance at 970 nm to the reflectance at 900 nm. Finally, the WBI is calculated as the ratio of reflectance at 900 nm to the reflectance at 970 nm.

In addition, despite its recognizable higher precision, hyperspectral TIR remote sensing has still received little attention to date [235,297].

Hyperspectral sensors have been used in several studies for PWS assessment. In citrus, Zarco-Tejada, with a UAV-mounted micro-hyperspectral imager, was able to estimate the g_s and Ψ_{stem} by vegetation indices calculated in the VIS-NIR band (NDVI, TCARI, PRI, etc...) and chlorophyll fluorescence indices [298]. Several works on PWS estimation by hyperspectral images have been carried out on grapevine [269,295,299]. Matese et al. conducted the first evaluation of a UAV hyperspectral dataset on the entire vine ecosystem, using narrowband VIS and multivariate PLS regressions [300]. This study included assessments of

water status and vegetative parameters (such as total and lateral leaf area, pruning weight), as well as pomological and quality parameters. In 2023, Vasquez et al. used a machine learning approach to predict grapevine Ψ_{stem} from UAV-based hyperspectral imagery in the NIR-SWIR range at different phenological stages [301]. Again, an RF model was used to model the data and 10-fold cross-validation was used for evaluation. The authors were able to develop a predictive model of the Ψ_{stem} with RMSE = 0.12 MPa. Exhaustive results were also found on apple [302], cherry [303], and almond [304] trees.

An important consideration about hyperspectral sensing in general is the relatively high cost. Currently, due to their technological complexity, hyperspectral sensors are less affordable than multispectral sensors. Additionally, a higher level of expertise is required to handle and interpret hyperspectral data [292].

4. Combined Approaches of Proximal and Remote Sensing

The joint use of proximal and remote sensing technologies could provide more comprehensive information on orchard water status and facilitate the acquisition of irrigation needs in terms of timing and volumes. Field water availability may depend on several factors, e.g., the soil texture [305], chemical, and physical properties [306], leaf area [307], presence of cover crops [308], field microclimate [309], etc.

Data from remote sensing could provide useful insights into spatial variability by allowing adequate field mapping. In this way, it would be possible to strategically place proximal sensors according to the distinct zones of the field. In addition, during the irrigation season, the continuous acquisition of data from proximal sensors could expand throughout the orchard by developing appropriate predictive models from vegetation indices obtained via UAVs or satellites. The result would be the expansion of information in time and space. For these reasons, the combination of the two approaches (proximal and remote) may prove to be an efficient and sustainable system for irrigation scheduling, greatly increasing water savings. Yet, as of now, affording a comprehensive system that integrates data from both proximal and remote sensors remains economically challenging for a significant portion of the agricultural community. For this reason, new low-cost sensors are continually being developed and validated, in part due to the simplicity of setting up affordable electronic systems and in part to the advancement of validation techniques such as machine learning. Furthermore, the UAV industry is making rapid progress towards producing miniaturized and cost-effective devices. Similarly, the accessibility and affordability of various satellite platforms could facilitate the retrieval of remote data.

To date, there is not a large number of studies combining remote and proximal sensing. Caruso et al. evaluated the combined use of multispectral data from UAVs with data from soil electrical conductivity sensors in order to identify homogeneous zone in a high-density irrigated olive orchard [265]. The authors found that the impact of various irrigation strategies on tree performance and water use efficiency (WUE) is location-dependent within the orchard, and tree vigor emerges as a primary factor influencing the ultimate fruit yield when the soil water availability is optimal. Matese et al. combined ground-based infrared thermography and thermal imaging from UAVs [310]. The results showed that CWSI values obtained from both remote and proximal sensors serve as useful indicators for evaluating the spatial variability in crop water status in Mediterranean vineyards. In almond, Gonzalez-Dugo et al. related the actual transpiration measured with heat-pulse sap flow probes with the CWSI, calculated using an empirical non-water stress baseline [311]. The relationship obtained between the CWSI and relative transpiration was high ($R^2 = 0.69$), demonstrating the effectiveness of the combined use of sap flow probes with airborne thermal imaging. To further confirm their combined use, a relationship between the CWSI and transpiration calculated from the sap flow output was also found on 'Tonda Romana' hazelnut (*Corylus avellana* L.) by Pasqualotto et al. [312]. No further coupling studies were found between remote sensing techniques and the proximal sensors mentioned above.

5. Conclusions

The management of irrigation water in orchards has become a crucial issue. Today, thanks to the techniques mentioned in this review, it is possible to develop an efficient and sustainable irrigation plan. As shown above, several types of sensors can prove useful in estimating PWS, but the future challenge lies in being able to find the appropriate combination for the crop type, soil, and climate. The integration of remote and plant-based proximal sensing techniques can effectively provide large-scale (time and space) information for the efficient monitoring of orchard water availability. However, few studies have investigated the combination of both techniques.

Developing appropriate protocols for efficient and sustainable irrigation management remains a primary research goal. Artificial intelligence may be an effective tool for the integration of different sensors, leading to new machine learning algorithms that can easily make system automation possible. Another challenge lies in the choice of sensors to be combined. An efficient and sustainable precision irrigation system should incorporate sensors that not only provide qualitative information about irrigation timing, but also offer quantitative data on plant water usage. One hypothesis is to combine sensors that provide direct information on water status (e.g., microtensiometers, psychrometers) with sensors that can monitor the response of various plant organs to different hydration levels (e.g., leaf turgor sensors and fruit gauges), and finally, those that can provide information on actual water consumption (e.g., sap flow sensors, leaf transpiration sensors).

Furthermore, integrating proximal systems with remote sensing can offer comprehensive information for more precise and efficient irrigation management, thereby minimizing water waste, meeting plant requirements, and maintaining good yields. Moreover, such accurate information would more easily enable an increasingly punctual irrigation system within orchards, which would lead to significant water savings, increased profits, and improved environmental sustainability. In addition to system precision, economic factors must also be considered. Nowadays, thanks to the more affordable prices of electronic components along with continuously evolving artificial intelligence tools, obtaining sensors and models that overcome the high costs associated with precision systems may become possible. Therefore, improving existing systems that have high potential but also high costs (e.g., microtensiometers, sap flow sensors) and making them accessible to a wide range of producers could be an immediate challenge. Regarding remote sensing systems, the prices of drones and satellite imagery are progressively decreasing, and such expenses can represent an investment to significantly increase profits.

This review provides updates on both proximal and remote sensing methodologies, encompassing established techniques like LPCP probes, fruit gauges, and sap flow probes as well as emerging technologies like microtensiometers, and potentially reliable and user-friendly options such as LWM and LMCP. In particular, the affordability of the latter is emphasized, as it would make it easily accessible to farmers. It is crucial to note the ongoing evolution of remote sensing methodologies, facilitated by the growing accessibility of instruments like UAVs, satellite platforms, and nanotechnologies. The final challenge launched by this review is to encourage researchers to investigate these techniques further and develop appropriate protocols that could make these methodologies increasingly accurate, reliable, and low-cost.

Author Contributions: Conceptualization, A.C. and R.L.B.; methodology, A.C.; investigation, A.C.; resources, A.C., P.T.B.F., R.L.B. and R.M.; data curation, A.C. and R.L.B.; writing—original draft preparation, A.C., P.T.B.F., R.M. and R.L.B.; writing—review and editing, A.C., P.T.B.F., R.L.B. and R.M.; visualization, A.C., R.M. and P.T.B.F.; supervision, R.L.B. and R.M.; funding acquisition, R.L.B. and R.M. All authors have read and agreed to the published version of the manuscript.

Funding: The present study was funded by the projects: Ecosistema dell'innovazione Sicilian MicronanoTech Research and Innovation Center—SAMOTHRACE. Fondo Finalizzato alla Ricerca di Ateneo FFR_D13_008811, funder: Ministero dell'Università e della Ricerca (MUR). European Project H2020-MSCA-RISE-2020—ref. 101007702, funder: European Commission—European Union.

Data Availability Statement: No new data were created or analyzed in this study. Data sharing is not applicable to this article.

Conflicts of Interest: The authors declare no conflicts of interest.

References

- Mirdashtvan, M.; Najafinejad, A.; Malekian, A.; Sa'doddin, A. Sustainable Water Supply and Demand Management in Semi-Arid Regions: Optimizing Water Resources Allocation Based on RCPs Scenarios. *Water Resour. Manag.* **2021**, *35*, 5307–5324. [[CrossRef](#)]
- Velasco-Muñoz, J.F.; Aznar-Sánchez, J.A.; Belmonte-Ureña, L.J.; Román-Sánchez, I.M. Sustainable Water Use in Agriculture: A Review of Worldwide Research. *Sustainability* **2018**, *10*, 1084. [[CrossRef](#)]
- Gosling, S.N.; Arnell, N.W. A Global Assessment of the Impact of Climate Change on Water Scarcity. *Clim. Chang.* **2016**, *134*, 371–385. [[CrossRef](#)]
- Del Pozo, A.; Brunel-Saldias, N.; Engler, A.; Ortega-Farias, S.; Acevedo-Opazo, C.; Lobos, G.A.; Jara-Rojas, R.; Molina-Montenegro, M.A. Climate Change Impacts and Adaptation Strategies of Agriculture in Mediterranean-Climate Regions (MCRs). *Sustainability* **2019**, *11*, 2769. [[CrossRef](#)]
- Webb, L.; Whiting, J.; Watt, A.; Hill, T.; Wigg, F.; Dunn, G.; Needs, S.; Barlow, E. Managing Grapevines through Severe Heat: A Survey of Growers after the 2009 Summer Heatwave in South-Eastern Australia. *J. Wine Res.* **2010**, *21*, 147–165. [[CrossRef](#)]
- Gautam, D.; Pagay, V. A Review of Current and Potential Applications of Remote Sensing to Study the Water Status of Horticultural Crops. *Agronomy* **2020**, *10*, 140. [[CrossRef](#)]
- Hristov, J.; Barreiro-Hurle, J.; Salputra, G.; Blanco, M.; Witzke, P. Reuse of Treated Water in European Agriculture: Potential to Address Water Scarcity under Climate Change. *Agric. Water Manag.* **2021**, *251*, 106872. [[CrossRef](#)] [[PubMed](#)]
- Allen, C.D.; Macalady, A.K.; Chenchouni, H.; Bachelet, D.; McDowell, N.; Vennetier, M.; Kitzberger, T.; Rigling, A.; Breshears, D.D.; Hogg, E.T. A Global Overview of Drought and Heat-Induced Tree Mortality Reveals Emerging Climate Change Risks for Forests. *For. Ecol. Manag.* **2010**, *259*, 660–684. [[CrossRef](#)]
- Fernández, J.E. Plant-Based Methods for Irrigation Scheduling of Woody Crops. *Horticulturae* **2017**, *3*, 35. [[CrossRef](#)]
- Noun, G.; Lo Cascio, M.; Spano, D.; Marras, S.; Sirca, C. Plant-Based Methodologies and Approaches for Estimating Plant Water Status of Mediterranean Tree Species: A Semi-Systematic Review. *Agronomy* **2022**, *12*, 2127. [[CrossRef](#)]
- Allen, R.G.; Pereira, L.S.; Raes, D.; Smith, M. Crop Evapotranspiration-Guidelines for Computing Crop Water Requirements-FAO Irrigation and Drainage Paper 56. *Fao Rome* **1998**, *300*, D05109.
- Cammalleri, C.; Ciraolo, G.; Minacapilli, M.; Rallo, G. Evapotranspiration from an Olive Orchard Using Remote Sensing-Based Dual Crop Coefficient Approach. *Water Resour. Manag.* **2013**, *27*, 4877–4895. [[CrossRef](#)]
- Allen, R.G.; Pereira, L.S. Estimating Crop Coefficients from Fraction of Ground Cover and Height. *Irrig. Sci.* **2009**, *28*, 17–34. [[CrossRef](#)]
- Jones, H.G. Monitoring Plant and Soil Water Status: Established and Novel Methods Revisited and Their Relevance to Studies of Drought Tolerance. *J. Exp. Bot.* **2007**, *58*, 119–130. [[CrossRef](#)] [[PubMed](#)]
- Paramasivam, S.; Alva, A.; Fares, A. An Evaluation of Soil Water Status Using Tensiometers in a Sandy Soil Profile under Citrus Production1. *Soil Sci.* **2000**, *165*, 343–353. [[CrossRef](#)]
- Coolong, T.; Snyder, J.; Warner, R.; Strang, J.; Surendran, S. The Relationship between Soil Water Potential, Environmental Factors, and Plant Moisture Status for Poblano Pepper Grown Using Tensiometer-Scheduled Irrigation. *Int. J. Veg. Sci.* **2012**, *18*, 137–152. [[CrossRef](#)]
- So, H. Water Potential Gradients and Resistances of a Soil-Root System Measured with the Root and Soil Psychrometer. In *The Soil-Root Interface*; Elsevier: Amsterdam, The Netherlands, 1979; pp. 99–113.
- Savage, M.J.; Ritchie, J.T.; Bland, W.L.; Dugas, W.A. Lower Limit of Soil Water Availability. *Agron. J.* **1996**, *88*, 644–651. [[CrossRef](#)]
- Payero, J.O.; Qiao, X.; Khalilian, A.; Mirzakhani-Nafchi, A.; Davis, R. Evaluating the Effect of Soil Texture on the Response of Three Types of Sensors Used to Monitor Soil Water Status. *J. Water Resour. Prot.* **2017**, *9*, 566. [[CrossRef](#)]
- Intrigliolo, D.S.; Castel, J.R. Continuous Measurement of Plant and Soil Water Status for Irrigation Scheduling in Plum. *Irrig. Sci.* **2004**, *23*, 93–102. [[CrossRef](#)]
- Ines, A.V.; Das, N.N.; Hansen, J.W.; Njoku, E.G. Assimilation of Remotely Sensed Soil Moisture and Vegetation with a Crop Simulation Model for Maize Yield Prediction. *Remote Sens. Environ.* **2013**, *138*, 149–164. [[CrossRef](#)]
- Mohanty, B.P.; Cosh, M.H.; Lakshmi, V.; Montzka, C. Soil Moisture Remote Sensing: State-of-the-Science. *Vadose Zone J.* **2017**, *16*, 1–9. [[CrossRef](#)]
- Schmitz, M.; Sourell, H. Variability in Soil Moisture Measurements. *Irrig. Sci.* **2000**, *19*, 147–151. [[CrossRef](#)]
- McCutchan, H.; Shackel, K. Stem-Water Potential as a Sensitive Indicator of Water Stress in Prune Trees (*Prunus domestica* L. Cv. French). *J. Am. Soc. Hort. Sci.* **1992**, *117*, 607–611. [[CrossRef](#)]
- Jones, H.G. Irrigation Scheduling: Advantages and Pitfalls of Plant-Based Methods. *J. Exp. Bot.* **2004**, *55*, 2427–2436. [[CrossRef](#)] [[PubMed](#)]
- Scalisi, A.; Bresilla, K.; Simões Grilo, F. Continuous Determination of Fruit Tree Water-Status by Plant-Based Sensors. *Italus Hortus* **2017**, *24*, 39–50. [[CrossRef](#)]

27. Shackel, K.A.; Ahmadi, H.; Biasi, W.; Buchner, R.; Goldhamer, D.; Gurusinghe, S.; Hasey, J.; Kester, D.; Krueger, B.; Lampinen, B. Plant Water Status as an Index of Irrigation Need in Deciduous Fruit Trees. *HortTechnology* **1997**, *7*, 23–29. [[CrossRef](#)]
28. Poblete-Echeverría, C.; Ortega-Farías, S.; Lobos, G.; Romero, S.; Ahumada, L.; Escobar, A.; Fuentes, S. Non-Invasive Method to Monitor Plant Water Potential of an Olive Orchard Using Visible and near Infrared Spectroscopy Analysis. *Acta Hort.* **2014**, *1057*, 363–368. [[CrossRef](#)]
29. Zimmermann, D.; Reuss, R.; Westhoff, M.; Gessner, P.; Bauer, W.; Bamberg, E.; Bentrup, F.-W.; Zimmermann, U. A Novel, Non-Invasive, Online-Monitoring, Versatile and Easy Plant-Based Probe for Measuring Leaf Water Status. *J. Exp. Bot.* **2008**, *59*, 3157–3167. [[CrossRef](#)] [[PubMed](#)]
30. Bennett, J.; Boote, K.; Hammond, L. Alterations in the Components of Peanut Leaf Water Potential during Desiccation. *J. Exp. Bot.* **1981**, *32*, 1035–1043. [[CrossRef](#)]
31. Lo Bianco, R.; Scalisi, A. Water Relations and Carbohydrate Partitioning of Four Greenhouse-Grown Olive Genotypes under Long-Term Drought. *Trees* **2017**, *31*, 717–727. [[CrossRef](#)]
32. Barrs, H.; Weatherley, P. A Re-Examination of the Relative Turgidity Technique for Estimating Water Deficits in Leaves. *Aust. J. Biol. Sci.* **1962**, *15*, 413–428. [[CrossRef](#)]
33. Dichio, B.; Xiloyannis, C.; Sofo, A.; Montanaro, G. Osmotic Regulation in Leaves and Roots of Olive Trees during a Water Deficit and Rewatering. *Tree Physiol.* **2006**, *26*, 179–185. [[CrossRef](#)]
34. Mullan, D.; Pietragalla, J. Leaf Relative Water Content. *Physiol. Breed. II Field Guide Wheat Phenotyping* **2012**, *25*, 25–27.
35. Tardieu, F.; Davies, W. Integration of Hydraulic and Chemical Signalling in the Control of Stomatal Conductance and Water Status of Droughted Plants. *Plant Cell Environ.* **1993**, *16*, 341–349. [[CrossRef](#)]
36. Whitehead, D. Assessment of Water Status in Trees from Measurements of Stomatal Conductance and Water Potential. *NZJ Sci.* **1980**, *10*, 159–165.
37. McBurney, T. The Relationship between Leaf Thickness and Plant Water Potential. *J. Exp. Bot.* **1992**, *43*, 327–335. [[CrossRef](#)]
38. Sakuratani, T. A Heat Balance Method for Measuring Water Flux in the Stem of Intact Plants. *J. Agric. Meteorol.* **1981**, *37*, 9–17. [[CrossRef](#)]
39. Escalona, J.; Flexas, J.; Medrano, H. Drought Effects on Water Flow, Photosynthesis and Growth of Potted Grapevines. *VITIS-GEILWEILERHOF* **2002**, *41*, 57–62.
40. Huck, M.G.; Klepper, B. Water Relations of Cotton. II. Continuous Estimates of Plant Water Potential from Stem Diameter Measurements. *Agron. J.* **1977**, *69*, 593–597. [[CrossRef](#)]
41. Intrigliolo, D.; Castel, J. Evaluation of Grapevine Water Status from Trunk Diameter Variations. *Irrig. Sci.* **2007**, *26*, 49–59. [[CrossRef](#)]
42. Doltra, J.; Oncins, J.A.; Bonany, J.; Cohen, M. Evaluation of Plant-Based Water Status Indicators in Mature Apple Trees under Field Conditions. *Irrig. Sci.* **2007**, *25*, 351–359. [[CrossRef](#)]
43. Ji, W.; Li, L.; Zhou, W. Design and Implementation of a RFID Reader/Router in RFID-WSN Hybrid System. *Future Internet* **2018**, *10*, 106. [[CrossRef](#)]
44. Mekonnen, Y.; Namuduri, S.; Burton, L.; Sarwat, A.; Bhansali, S. Machine Learning Techniques in Wireless Sensor Network Based Precision Agriculture. *J. Electrochem. Soc.* **2019**, *167*, 037522. [[CrossRef](#)]
45. Alexopoulos, A.; Koutras, K.; Ali, S.B.; Puccio, S.; Carella, A.; Ottaviano, R.; Kalogerias, A. Complementary Use of Ground-Based Proximal Sensing and Airborne/Spaceborne Remote Sensing Techniques in Precision Agriculture: A Systematic Review. *Agronomy* **2023**, *13*, 1942. [[CrossRef](#)]
46. Roma, E.; Catania, P. Precision Oliviculture: Research Topics, Challenges, and Opportunities—A Review. *Remote Sens.* **2022**, *14*, 1668. [[CrossRef](#)]
47. Asgari, N.; Ayoubi, S.; Jafari, A.; Demattê, J.A. Incorporating Environmental Variables, Remote and Proximal Sensing Data for Digital Soil Mapping of USDA Soil Great Groups. *Int. J. Remote Sens.* **2020**, *41*, 7624–7648. [[CrossRef](#)]
48. Damásio, M.; Barbosa, M.; Deus, J.; Fernandes, E.; Leitão, A.; Albino, L.; Fonseca, F.; Silvestre, J. Can Grapevine Leaf Water Potential Be Modelled from Physiological and Meteorological Variables? A Machine Learning Approach. *Plants* **2023**, *12*, 4142. [[CrossRef](#)]
49. Thoday, D. On the Water Relations of Plant Cells. *Ann. Bot.* **1950**, *14*, 1–6. [[CrossRef](#)]
50. Wenkert, W.; Lemon, E.; Sinclair, T. Leaf Elongation and Turgor Pressure in Field-grown Soybean. *Agron. J.* **1978**, *70*, 761–764. [[CrossRef](#)]
51. Rodríguez-Dominguez, C.M.; Buckley, T.N.; Egea, G.; de Cires, A.; Hernandez-Santana, V.; Martorell, S.; Diaz-Espejo, A. Most Stomatal Closure in Woody Species under Moderate Drought Can Be Explained by Stomatal Responses to Leaf Turgor. *Plant Cell Environ.* **2016**, *39*, 2014–2026. [[CrossRef](#)]
52. Zimmermann, U.; Rüger, S.; Shapira, O.; Westhoff, M.; Wegner, L.; Reuss, R.; Gessner, P.; Zimmermann, G.; Israeli, Y.; Zhou, A. Effects of Environmental Parameters and Irrigation on the Turgor Pressure of Banana Plants Measured Using the Non-invasive, Online Monitoring Leaf Patch Clamp Pressure Probe. *Plant Biol.* **2010**, *12*, 424–436. [[CrossRef](#)]
53. Green, P.B.; Stanton, F.W. Turgor Pressure: Direct Manometric Measurement in Single Cells of *Nitella*. *Science* **1967**, *155*, 1675–1676. [[CrossRef](#)] [[PubMed](#)]
54. Zimmermann, U.; Råde, H.; Steudle, E. Kontinuierliche Druckmessung in Pflanzenzellen. *Naturwissenschaften* **1969**, *56*, 634. [[CrossRef](#)]

55. Steudle, E.; Zimmermann, U.; Lüttge, U. Effect of Turgor Pressure and Cell Size on the Wall Elasticity of Plant Cells. *Plant Physiol.* **1977**, *59*, 285–289. [[CrossRef](#)] [[PubMed](#)]
56. Hüsken, D.; Steudle, E.; Zimmermann, U. Pressure Probe Technique for Measuring Water Relations of Cells in Higher Plants. *Plant Physiol.* **1978**, *61*, 158–163. [[CrossRef](#)] [[PubMed](#)]
57. Howard, R.J.; Ferrari, M.A.; Roach, D.H.; Money, N.P. Penetration of Hard Substrates by a Fungus Employing Enormous Turgor Pressures. *Proc. Natl. Acad. Sci. USA* **1991**, *88*, 11281–11284. [[CrossRef](#)] [[PubMed](#)]
58. Marino, G.; Scalisi, A.; Guzmán-Delgado, P.; Caruso, T.; Marra, F.P.; Lo Bianco, R. Detecting Mild Water Stress in Olive with Multiple Plant-Based Continuous Sensors. *Plants* **2021**, *10*, 131. [[CrossRef](#)] [[PubMed](#)]
59. Marino, G.; Pernice, F.; Marra, F.P.; Caruso, T. Validation of an Online System for the Continuous Monitoring of Tree Water Status for Sustainable Irrigation Managements in Olive (*Olea europaea* L.). *Agric. Water Manag.* **2016**, *177*, 298–307. [[CrossRef](#)]
60. Padilla-Díaz, C.; Rodríguez-Domínguez, C.; Hernández-Santana, V.; Pérez-Martin, A.; Fernández, J. Scheduling Regulated Deficit Irrigation in a Hedgerow Olive Orchard from Leaf Turgor Pressure Related Measurements. *Agric. Water Manag.* **2016**, *164*, 28–37. [[CrossRef](#)]
61. Ehrenberger, W.; Rüger, S.; Rodríguez-Domínguez, C.M.; Díaz-Espejo, A.; Fernández, J.E.; Moreno, J.; Zimmermann, D.; Sukhorukov, V.L.; Zimmermann, U. Leaf Patch Clamp Pressure Probe Measurements on Olive Leaves in a Nearly Turgorless State. *Plant Biol.* **2012**, *14*, 666–674. [[CrossRef](#)]
62. Rüger, S.; Netzer, Y.; Westhoff, M.; Zimmermann, D.; Reuss, R.; Ovadiya, S.; Gessner, P.; Zimmermann, G.; Schwartz, A.; Zimmermann, U. Remote Monitoring of Leaf Turgor Pressure of Grapevines Subjected to Different Irrigation Treatments Using the Leaf Patch Clamp Pressure Probe. *Aust. J. Grape Wine Res.* **2010**, *16*, 405–412. [[CrossRef](#)]
63. Westhoff, M.; Zimmermann, D.; Zimmermann, G.; Gessner, P.; Wegner, L.; Bentrup, F.-W.; Zimmermann, U. Distribution and Function of Epistomatal Mucilage Plugs. *Protoplasma* **2009**, *235*, 101–105. [[CrossRef](#)] [[PubMed](#)]
64. Scalisi, A.; O’Connell, M.G.; Stefanelli, D.; Lo Bianco, R. Fruit and Leaf Sensing for Continuous Detection of Nectarine Water Status. *Front. Plant Sci.* **2019**, *10*, 805. [[CrossRef](#)] [[PubMed](#)]
65. Scalisi, A.; O’Connell, M.; Lo Bianco, R.; Stefanelli, D. Continuous Detection of New Plant Water Status Indicators in Stage I of Nectarine Fruit Growth. In Proceedings of the XXX International Horticultural Congress IHC2018: International Symposium on Water and Nutrient Relations and Management of Horticultural Crops, Istanbul, Turkey, 12–16 August 2018; pp. 9–16.
66. Ballester, C.; Castiella, M.; Zimmermann, U.; Rüger, S.; Martínez Gimeno, M.A.; Intrigliolo, D.S. Usefulness of the ZIM-Probe Technology for Detecting Water Stress in Clementine and Persimmon Trees. In Proceedings of the VIII International Symposium on Irrigation of Horticultural Crops, Lleida, Spain, 8–11 June 2015; pp. 105–112.
67. Martínez-Gimeno, M.A.; Castiella, M.; Rüger, S.; Intrigliolo, D.S.; Ballester, C. Evaluating the Usefulness of Continuous Leaf Turgor Pressure Measurements for the Assessment of Persimmon Tree Water Status. *Irrig. Sci.* **2017**, *35*, 159–167. [[CrossRef](#)]
68. Scalisi, A.; Marino, G.; Marra, F.P.; Caruso, T.; Lo Bianco, R. A Cultivar-Sensitive Approach for the Continuous Monitoring of Olive (*Olea europaea* L.) Tree Water Status by Fruit and Leaf Sensing. *Front. Plant Sci.* **2020**, *11*, 340. [[CrossRef](#)] [[PubMed](#)]
69. Massenti, R.; Scalisi, A.; Marra, F.P.; Caruso, T.; Marino, G.; Lo Bianco, R. Physiological and Structural Responses to Prolonged Water Deficit in Young Trees of Two Olive Cultivars. *Plants* **2022**, *11*, 1695. [[CrossRef](#)] [[PubMed](#)]
70. Fernández, J.; Rodríguez-Domínguez, C.; Pérez-Martin, A.; Zimmermann, U.; Rüger, S.; Martín-Palomo, M.; Torres-Ruiz, J.; Cuevas, M.; Sann, C.; Ehrenberger, W. Online-Monitoring of Tree Water Stress in a Hedgerow Olive Orchard Using the Leaf Patch Clamp Pressure Probe. *Agric. Water Manag.* **2011**, *100*, 25–35. [[CrossRef](#)]
71. Sghaier, A.; Chehab, H.; Aissaoui, F.; Naggaz, K.; Ouessar, M.; Boujnah, D. Effect of Three Irrigation Frequencies on Physiological-Biological Aspects of Young Olive Trees (*Olea europaea* L. Cvs’ Koroneiki’ and ‘Picholine’): Vegetative Growth, Leaf Turgor Pressure, and Fluorescence. *Pol. J. Environ. Stud.* **2019**, *28*, 23632370. [[CrossRef](#)]
72. Barriga, J.A.; Blanco-Cipollone, F.; Trigo-Córdoba, E.; García-Tejero, I.; Clemente, P.J. Crop-water assessment in Citrus (*Citrus sinensis* L.) based on continuous measurements of leaf-turgor pressure using machine learning and IoT. *Expert Syst. Appl.* **2022**, *209*, 118255. [[CrossRef](#)]
73. Palomo, J.; Romero, R.; Cuevas, M.V.; Alamo, T.; Muñoz de la Peña, D. Water Stress Estimation from Leaf Turgor Pressure in Arbequina Olive Orchards Based on Linear Discriminant Analysis. *Exp. Syst. Appl.* **2024**, preprint submitted. Available online: <https://ssrn.com/abstract=4719404> (accessed on 15 May 2024).
74. Cecilia, B.; Francesca, A.; Dalila, P.; Carlo, S.; Antonella, G.; Francesco, F.; Marco, R.; Mauro, C. On-Line Monitoring of Plant Water Status: Validation of a Novel Sensor Based on Photon Attenuation of Radiation through the Leaf. *Sci. Total Environ.* **2022**, *817*, 152881. [[CrossRef](#)]
75. Kaiser, H. A New Device for Continuous Non-Invasive Measurements of Leaf Water Content Using NIR-Transmission Allowing Dynamic Tracking of Water Budgets. *bioRxiv* **2022**, preprint submitted. Available online: <https://www.biorxiv.org/content/10.1101/2022.05.06.490892v1> (accessed on 15 May 2024). [[CrossRef](#)]
76. Haworth, M.; Marino, G.; Atzori, G.; Fabbri, A.; Daccache, A.; Killi, D.; Carli, A.; Montesano, V.; Conte, A.; Balestrini, R. Plant Physiological Analysis to Overcome Limitations to Plant Phenotyping. *Plants* **2023**, *12*, 4015. [[CrossRef](#)] [[PubMed](#)]
77. Meidner, H. An Instrument for the Continuous Determination of Leaf Thickness Changes in the Field. *J. Exp. Bot.* **1952**, *3*, 319–325. [[CrossRef](#)]
78. Scoffoni, C.; Vuong, C.; Diep, S.; Cochard, H.; Sack, L. Leaf Shrinkage with Dehydration: Coordination with Hydraulic Vulnerability and Drought Tolerance. *Plant Physiol.* **2014**, *164*, 1772–1788. [[CrossRef](#)] [[PubMed](#)]

79. Seelig, H.-D.; Stoner, R.J.; Linden, J.C. Irrigation Control of Cowpea Plants Using the Measurement of Leaf Thickness under Greenhouse Conditions. *Irrig. Sci.* **2012**, *30*, 247–257. [[CrossRef](#)]
80. Rozema, J.; van Arp, W.; van Diggelen, J.; Kok, E.; Letschert, J. An Ecophysiological Comparison of Measurements of the Diurnal Rhythm of the Leaf Elongation and Changes of the Leaf Thickness of Salt-Resistant Dicotyledonae and Monocotyledonae. *J. Exp. Bot.* **1987**, *38*, 442–453. [[CrossRef](#)]
81. Burquez, A. Leaf Thickness and Water Deficit in Plants: A Tool for Field Studies. *J. Exp. Bot.* **1987**, *38*, 109–114. [[CrossRef](#)]
82. Giuliani, R.; Koteyeva, N.; Voznesenskaya, E.; Evans, M.A.; Cousins, A.B.; Edwards, G.E. Coordination of Leaf Photosynthesis, Transpiration, and Structural Traits in Rice and Wild Relatives (Genus *Oryza*). *Plant Physiol.* **2013**, *162*, 1632–1651. [[CrossRef](#)]
83. Afzal, A.; Duiker, S.W.; Watson, J.E. Leaf Thickness to Predict Plant Water Status. *Biosyst. Eng.* **2017**, *156*, 148–156. [[CrossRef](#)]
84. Bachmann, F. Studien Über Dickenänderungen von Laubblättern. *Jb Wiss. Bot.* **1922**, *61*, 372–429.
85. Malone, M. Kinetics of Wound-Induced Hydraulic Signals and Variation Potentials in Wheat Seedlings. *Planta* **1992**, *187*, 505–510. [[CrossRef](#)]
86. Jinwen, L.; Jingping, Y.; Pinpin, F.; Junlan, S.; Dongsheng, L.; Changshui, G.; Wenyue, C. Responses of Rice Leaf Thickness, SPAD Readings and Chlorophyll a/b Ratios to Different Nitrogen Supply Rates in Paddy Field. *Field Crops Res.* **2009**, *114*, 426–432. [[CrossRef](#)]
87. Sharon, Y.; Bravdo, B.-A. Irrigation Control for Citrus According to the Diurnal Cycling of Leaf Thickness. In Proceedings of the International Conference on Water & Irrigation, Tel Aviv, Israel, 13–16 May 1996; pp. 273–283.
88. Thalheimer, M. A Leaf-Mounted Capacitance Sensor for Continuous Monitoring of Foliar Transpiration and Solar Irradiance as an Indicator of Plant Water Status. *J. Agric. Eng.* **2023**, *54*. [[CrossRef](#)]
89. Moreshet, S.; Yocum, C. A Condensation Type Porometer for Field Use. *Plant Physiol.* **1972**, *49*, 944–949. [[CrossRef](#)] [[PubMed](#)]
90. Miner, G.L.; Ham, J.M.; Kluitenberg, G.J. A Heat-Pulse Method for Measuring Sap Flow in Corn and Sunflower Using 3D-Printed Sensor Bodies and Low-Cost Electronics. *Agric. For. Meteorol.* **2017**, *246*, 86–97. [[CrossRef](#)]
91. Afzal, A.; Duiker, S.W.; Watson, J.E.; Luthe, D. Leaf Thickness and Electrical Capacitance as Measures of Plant Water Status. *Trans. ASABE* **2017**, *60*, 1063–1074. [[CrossRef](#)]
92. Arve, L.E.; Kruse, O.M.O.; Tanino, K.K.; Olsen, J.E.; Futsæther, C.; Torre, S. Daily Changes in VPD during Leaf Development in High Air Humidity Increase the Stomatal Responsiveness to Darkness and Dry Air. *J. Plant Physiol.* **2017**, *211*, 63–69. [[CrossRef](#)] [[PubMed](#)]
93. Maroco, J.P.; Pereira, J.S.; Chaves, M.M. Stomatal Responses to Leaf-to-Air Vapour Pressure Deficit in Sahelian Species. *Funct. Plant Biol.* **1997**, *24*, 381–387. [[CrossRef](#)]
94. McAdam, S.A.; Brodribb, T.J. The Evolution of Mechanisms Driving the Stomatal Response to Vapor Pressure Deficit. *Plant Physiol.* **2015**, *167*, 833–843. [[CrossRef](#)] [[PubMed](#)]
95. Clauser, L. Precision Water Management in Apple Orchards: Comparison of Technologies. Master’s Thesis, University of Padua, Padua, Italy, 26 February 2024.
96. Jackson, R.D.; Idso, S.; Reginato, R.; Pinter, P., Jr. Canopy Temperature as a Crop Water Stress Indicator. *Water Resour. Res.* **1981**, *17*, 1133–1138. [[CrossRef](#)]
97. Leinonen, I.; Jones, H.G. Combining Thermal and Visible Imagery for Estimating Canopy Temperature and Identifying Plant Stress. *J. Exp. Bot.* **2004**, *55*, 1423–1431. [[CrossRef](#)]
98. Idso, S.; Jackson, R.; Pinter, P., Jr.; Reginato, R.; Hatfield, J. Normalizing the Stress-Degree-Day Parameter for Environmental Variability. *Agric. Meteorol.* **1981**, *24*, 45–55. [[CrossRef](#)]
99. Yu, L.; Wang, W.; Zhang, X.; Zheng, W. *A Review on Leaf Temperature Sensor: Measurement Methods and Application*; Springer: Berlin/Heidelberg, Germany, 2016; pp. 216–230.
100. Kim, B. Assessing Accuracy over Warm-up Time of Lepton 3.5 Thermal Imaging for Measuring Leaf Temperature of Crops. *J. Appl. Hortic.* **2023**, *25*, 39–42. [[CrossRef](#)]
101. Kim, B. Feasibility of Lepton 3.5 Using Warm-Up Time for Measuring Leaf Temperature of Crops. 2023, preprint submitted. Available online: <https://www.researchsquare.com/article/rs-2707772/v1> (accessed on 15 May 2024). [[CrossRef](#)]
102. Atherton, J.J.; Rosamond, M.C.; Zeze, D.A. A Leaf-Mounted Thermal Sensor for the Measurement of Water Content. *Sens. Actuators Phys.* **2012**, *187*, 67–72. [[CrossRef](#)]
103. Adachi, H.; Uchida, K.; Saitoh, E.; Maekawa, S. Theory of the Spin Seebeck Effect. *Rep. Prog. Phys.* **2013**, *76*, 036501. [[CrossRef](#)]
104. Uchida, K.-I.; Takahashi, S.; Harii, K.; Ieda, J.; Koshibae, W.; Ando, K.; Maekawa, S.; Saitoh, E. Observation of the Spin Seebeck Effect. *Nature* **2008**, *455*, 778–781. [[CrossRef](#)] [[PubMed](#)]
105. Pou, A.; Diago, M.P.; Medrano, H.; Baluja, J.; Tardaguila, J. Validation of Thermal Indices for Water Status Identification in Grapevine. *Agric. Water Manag.* **2014**, *134*, 60–72. [[CrossRef](#)]
106. Costa, J.; Egipto, R.; Sánchez-Virosta, A.; Lopes, C.; Chaves, M. Canopy and Soil Thermal Patterns to Support Water and Heat Stress Management in Vineyards. *Agric. Water Manag.* **2019**, *216*, 484–496. [[CrossRef](#)]
107. Dhillon, R.S.; Upadhaya, S.K.; Rojo, F.; Roach, J.; Coates, R.W.; Delwiche, M.J. Development of a Continuous Leaf Monitoring System to Predict Plant Water Status. *Trans. ASABE* **2017**, *60*, 1445–1455. [[CrossRef](#)]
108. Dhillon, R.; Rojo, F.; Upadhaya, S.K.; Roach, J.; Coates, R.; Delwiche, M. Prediction of Plant Water Status in Almond and Walnut Trees Using a Continuous Leaf Monitoring System. *Precis. Agric.* **2019**, *20*, 723–745. [[CrossRef](#)]

109. Li, X.H.; Li, M.Z.; Li, J.Y.; Gao, Y.Y.; Liu, C.R.; Hao, G.F. Wearable sensor supports in-situ and continuous monitoring of plant health in precision agriculture era. *Plant Biotechnol. J.* **2024**, 1–20. [[CrossRef](#)]
110. Muthumalai, K.; Gokila, N.; Haldorai, Y.; Rajendra Kumar, R.T. Advanced Wearable Sensing Technologies for Sustainable Precision Agriculture—A Review on Chemical Sensors. *Adv. Sens. Res.* **2024**, 3, 2300107. [[CrossRef](#)]
111. Peng, B.; Liu, X.; Yao, Y.; Ping, J.; Ying, Y. A Wearable and Capacitive Sensor for Leaf Moisture Status Monitoring. *Biosens. Bioelectron.* **2024**, 245, 115804. [[CrossRef](#)] [[PubMed](#)]
112. Wang, Y.; Anderegg, W.R.; Venturas, M.D.; Trugman, A.T.; Yu, K.; Frankenberg, C. Optimization Theory Explains Nighttime Stomatal Responses. *New Phytol.* **2021**, 230, 1550–1561. [[CrossRef](#)] [[PubMed](#)]
113. Im, H.; Lee, S.; Naqi, M.; Lee, C.; Kim, S. Flexible PI-Based Plant Drought Stress Sensor for Real-Time Monitoring System in Smart Farm. *Electronics* **2018**, 7, 114. [[CrossRef](#)]
114. Fernández, J.; Cuevas, M. Irrigation Scheduling from Stem Diameter Variations: A Review. *Agric. For. Meteorol.* **2010**, 150, 135–151. [[CrossRef](#)]
115. Hinckley, T.M.; Bruckerhoff, D.N. The Effects of Drought on Water Relations and Stem Shrinkage of *Quercus Alba*. *Can. J. Bot.* **1975**, 53, 62–72. [[CrossRef](#)]
116. Čermák, J.; Kučera, J.; Bauerle, W.L.; Phillips, N.; Hinckley, T.M. Tree Water Storage and Its Diurnal Dynamics Related to Sap Flow and Changes in Stem Volume in Old-Growth Douglas-Fir Trees. *Tree Physiol.* **2007**, 27, 181–198. [[CrossRef](#)] [[PubMed](#)]
117. Genard, M.; Fishman, S.; Vercambre, G.; Huguet, J.-G.; Bussi, C.; Besset, J.; Habib, R. A Biophysical Analysis of Stem and Root Diameter Variations in Woody Plants. *Plant Physiol.* **2001**, 126, 188–202. [[CrossRef](#)]
118. Herzog, K.M.; Häslér, R.; Thum, R. Diurnal Changes in the Radius of a Subalpine Norway Spruce Stem: Their Relation to the Sap Flow and Their Use to Estimate Transpiration. *Trees* **1995**, 10, 94–101. [[CrossRef](#)]
119. Molz, F.J.; Klepper, B. On the Mechanism of Water-Stress-Induced Stem Deformation. *Agron. J.* **1973**, 65, 304–306. [[CrossRef](#)]
120. Molz, F.J.; Klepper, B.; Browning, V.D. Radial Diffusion of Free Energy in Stem Phloem: An Experimental Study. *Agron. J.* **1973**, 65, 219–222. [[CrossRef](#)]
121. Cochard, H.; Forestier, S.; Améglio, T. A New Validation of the Scholander Pressure Chamber Technique Based on Stem Diameter Variations. *J. Exp. Bot.* **2001**, 52, 1361–1365. [[CrossRef](#)] [[PubMed](#)]
122. Parlange, J.-Y.; Turner, N.C.; Waggoner, P.E. Water Uptake, Diameter Change, and Nonlinear Diffusion in Tree Stems. *Plant Physiol.* **1975**, 55, 247–250. [[CrossRef](#)] [[PubMed](#)]
123. Gallardo, M.; Thompson, R.; Valdez, L.; Fernández, M. Response of Stem Diameter Variations to Water Stress in Greenhouse-Grown Vegetable Crops. *J. Hortic. Sci. Biotechnol.* **2006**, 81, 483–495. [[CrossRef](#)]
124. Böhmerle, K. Die Pfister'sche Zuwachsuhr. *Zentralblatt Für Gesamte Forstwes* **1883**, 9, 83–93.
125. Kozłowski, T.; Winget, C. Diurnal and Seasonal Variation in Radii of Tree Stems. *Ecology* **1964**, 45, 149–155. [[CrossRef](#)]
126. Holmes, J.; Shim, S. Diurnal Changes in Stem Diameter of Canary Island Pine Trees (*Pinus canariensis*, C. Smith) Caused by Soil Water Stress and Varying Microclimate. *J. Exp. Bot.* **1968**, 19, 219–232. [[CrossRef](#)]
127. Valentini, R.; Belelli Marchesini, L.; Gianelle, D.; Sala, G.; Yarovslavtsev, A.; Vasenev, V.; Castaldi, S. New Tree Monitoring Systems: From Industry 4.0 to Nature 4.0. *Ann. Silv. Res.* **2019**, 43, 84–88.
128. Hao, G.-Y.; Wheeler, J.; Holbrook, N.; Goldstein, G.; Carrasco, L.; Bucci, S.; Scholz, F.; Campanello, P.; Madanes, N.; Cristiano, P. Water Storage Discharge and Refilling in the Main Stems of Canopy Tree Species Investigated Using Frequency Domain Reflectometry and Electronic Point Dendrometers. In Proceedings of the IX International Workshop on Sap Flow, Gent, Belgium, 4–7 June 2013; pp. 17–24.
129. Drew, D.M.; Downes, G.M. The Use of Precision Dendrometers in Research on Daily Stem Size and Wood Property Variation: A Review. *Dendrochronologia* **2009**, 27, 159–172. [[CrossRef](#)]
130. Naor, A.; Cohen, S. Sensitivity and Variability of Maximum Trunk Shrinkage, Midday Stem Water Potential, and Transpiration Rate in Response to Withholding Irrigation from Field-Grown Apple Trees. *HortScience* **2003**, 38, 547–551. [[CrossRef](#)]
131. Goldhamer, D.A.; Fereres, E.; Mata, M.; Girona, J.; Cohen, M. Sensitivity of Continuous and Discrete Plant and Soil Water Status Monitoring in Peach Trees Subjected to Deficit Irrigation. *J. Am. Soc. Hortic. Sci.* **1999**, 124, 437–444. [[CrossRef](#)]
132. Wheeler, W.D.; Black, B.; Bugbee, B. Assessing water stress in a high-density apple orchard using trunk circumference variation, sap flow index and stem water potential. *Front. Plant Sci.* **2023**, 14, 1214429. [[CrossRef](#)] [[PubMed](#)]
133. Conejero, W.; Alarcón, J.; García-Orellana, Y.; Nicolás, E.; Torrecillas, A. Evaluation of Sap Flow and Trunk Diameter Sensors for Irrigation Scheduling in Early Maturing Peach Trees. *Tree Physiol.* **2007**, 27, 1753–1759. [[CrossRef](#)] [[PubMed](#)]
134. Mirás-Avalos, J.M.; Pérez-Sarmiento, F.; Alcobendas, R.; Alarcón, J.J.; Mounzer, O.; Nicolás, E. Maximum Daily Trunk Shrinkage for Estimating Water Needs and Scheduling Regulated Deficit Irrigation in Peach Trees. *Irrig. Sci.* **2017**, 35, 69–82. [[CrossRef](#)]
135. De la Rosa, J.M.; Dodd, I.C.; Domingo, R.; Pérez-Pastor, A. Early Morning Fluctuations in Trunk Diameter Are Highly Sensitive to Water Stress in Nectarine Trees. *Irrig. Sci.* **2016**, 34, 117–128. [[CrossRef](#)]
136. Martín-Palomo, M.; Andreu, L.; Pérez-López, D.; Centeno, A.; Galindo, A.; Moriana, A.; Corell, M. Trunk Growth Rate Frequencies as Water Stress Indicator in Almond Trees. *Agric. Water Manag.* **2022**, 271, 107765. [[CrossRef](#)]
137. Vélez-Sánchez, J.E.; Balaguera-López, H.E.; Rodríguez Hernández, P. The Water Status of Pear (*Pyrus communis* L.) under Application of Regulated Deficit Irrigation in High Tropical Latitudinal Conditions. *J. Saudi Soc. Agric. Sci.* **2022**, 21, 460–468. [[CrossRef](#)]

138. Blanco, V.; Kalcsits, L. Long-Term Validation of Continuous Measurements of Trunk Water Potential and Trunk Diameter Indicate Different Diurnal Patterns for Pear under Water Limitations. *Agric. Water Manag.* **2023**, *281*, 108257. [CrossRef]
139. Corell, M.; Martín-Palomo, M.J.; Pérez-López, D.; Centeno, A.; Girón, I.; Moreno, F.; Torrecillas, A.; Moriana, A. Approach for Using Trunk Growth Rate (TGR) in the Irrigation Scheduling of Table Olive Orchards. *Agric. Water Manag.* **2017**, *192*, 12–20. [CrossRef]
140. Blanco, V.; Domingo, R.; Pérez-Pastor, A.; Blaya-Ros, P.J.; Torres-Sánchez, R. Soil and Plant Water Indicators for Deficit Irrigation Management of Field-Grown Sweet Cherry Trees. *Agric. Water Manag.* **2018**, *208*, 83–94. [CrossRef]
141. Conesa, M.R.; Dodd, I.C.; Temnani, A.; De la Rosa, J.M.; Pérez-Pastor, A. Physiological Response of Post-Veraison Deficit Irrigation Strategies and Growth Patterns of Table Grapes (Cv. Crimson Seedless). *Agric. Water Manag.* **2018**, *208*, 363–372. [CrossRef]
142. Pagay, V.; Santiago, M.; Sessoms, D.A.; Huber, E.J.; Vincent, O.; Pharkya, A.; Corso, T.N.; Lakso, A.N.; Stroock, A.D. A Microtensiometer Capable of Measuring Water Potentials Below –10 MPa. *Lab Chip* **2014**, *14*, 2806–2817. [CrossRef] [PubMed]
143. Black, W.L.; Santiago, M.; Zhu, S.; Stroock, A.D. Ex Situ and in Situ Measurement of Water Activity with a MEMS Tensiometer. *Anal. Chem.* **2019**, *92*, 716–723. [CrossRef] [PubMed]
144. Pagay, V. Evaluating a Novel Microtensiometer for Continuous Trunk Water Potential Measurements in Field-Grown Irrigated Grapevines. *Irrig. Sci.* **2022**, *40*, 45–54. [CrossRef]
145. Richards, L. Soil Moisture Tensiometer Materials and Construction. *Soil Sci.* **1942**, *53*, 241–248. [CrossRef]
146. Lakso, A.N.; Santiago, M.; Stroock, A.D. Monitoring Stem Water Potential with an Embedded Microtensiometer to Inform Irrigation Scheduling in Fruit Crops. *Horticulturae* **2022**, *8*, 1207. [CrossRef]
147. Zucchini, M.; Guzmán-Delgado, P.; Santos, E.; Synsteli, T.; Marino, G. Preliminary Observations on the Use of Microtensiometers to Continuously Measure Water Potential in a Mature Olive Orchard. In Proceedings of the 2023 IEEE International Workshop on Metrology for Agriculture and Forestry (MetroAgriFor), Pisa, Italy, 6–8 November 2023; pp. 268–272.
148. Conesa, M.R.; Conejero, W.; Vera, J.; Ruiz-Sánchez, M.C. Assessment of Trunk Microtensiometer as a Novel Biosensor to Continuously Monitor Plant Water Status in Nectarine Trees. *Front. Plant Sci.* **2023**, *14*, 1123045. [CrossRef] [PubMed]
149. Blanco, V.; Kalcsits, L. Microtensiometers Accurately Measure Stem Water Potential in Woody Perennials. *Plants* **2021**, *10*, 2780. [CrossRef] [PubMed]
150. Kisekka, I.; Peddinti, S.R.; Savchik, P.; Yang, L.; Culumber, M.; Bali, K.; Milliron, L.; Edwards, E.; Nocco, M.; Reyes, C.; et al. Multisite Evaluation of Microtensiometer and Osmotic Cell Stem Water Potential Sensors in Almond Orchards. 2024, preprint submitted. Available online: <https://ssrn.com/abstract=4713202> (accessed on 15 May 2024). [CrossRef]
151. Gonzalez Nieto, L.; Huber, A.; Gao, R.; Biasuz, E.C.; Cheng, L.; Stroock, A.D.; Lakso, A.N.; Robinson, T.L. Trunk Water Potential Measured with Microtensiometers for Managing Water Stress in “Gala” Apple Trees. *Plants* **2023**, *12*, 1912. [CrossRef]
152. Lakso, A.; Zhu, S.; Santiago, M.; Shackel, K.; Volkov, V.; Stroock, A. A Microtensiometer Sensor to Continuously Monitor Stem Water Potentials in Woody Plants Design and Field Testing. In Proceedings of the IX International Symposium on Irrigation of Horticultural Crops, Matera, Italy, 17–20 June 2019; pp. 317–324.
153. Marra, F.; Marino, G.; Marchese, A.; Caruso, T. Effects of Different Irrigation Regimes on a Super-High-Density Olive Grove Cv. “Arbequina”: Vegetative Growth, Productivity and Polyphenol Content of the Oil. *Irrig. Sci.* **2016**, *34*, 313–325. [CrossRef]
154. Granier, A.; Bréda, N. Modelling Canopy Conductance and Stand Transpiration of an Oak Forest from Sap Flow Measurements. *EDP Sci.* **1996**, *53*, 537–546. [CrossRef]
155. Smith, D.; Allen, S. Measurement of Sap Flow in Plant Stems. *J. Exp. Bot.* **1996**, *47*, 1833–1844. [CrossRef]
156. Poyatos, R.; Granda, V.; Molowny-Horas, R.; Mencuccini, M.; Steppe, K.; Martínez-Vilalta, J. SAPFLUXNET: Towards a Global Database of Sap Flow Measurements. *Tree Physiol.* **2016**, *36*, 1449–1455. [CrossRef] [PubMed]
157. Flo, V.; Martínez-Vilalta, J.; Steppe, K.; Schuldt, B.; Poyatos, R. A Synthesis of Bias and Uncertainty in Sap Flow Methods. *Agric. For. Meteorol.* **2019**, *271*, 362–374. [CrossRef]
158. Granier, A. Une Nouvelle Méthode Pour La Mesure Du Flux de Sève Brute Dans Le Tronc Des Arbres. *EDP Sci.* **1985**, *42*, 193–200. [CrossRef]
159. Do, F.; Rocheteau, A. Influence of Natural Temperature Gradients on Measurements of Xylem Sap Flow with Thermal Dissipation Probes. 1. Field Observations and Possible Remedies. *Tree Physiol.* **2002**, *22*, 641–648. [CrossRef] [PubMed]
160. Swanson, R.H.; Whitfield, D. A Numerical Analysis of Heat Pulse Velocity Theory and Practice. *J. Exp. Bot.* **1981**, *32*, 221–239. [CrossRef]
161. Burgess, S.S.; Adams, M.A.; Turner, N.C.; Beverly, C.R.; Ong, C.K.; Khan, A.A.; Bleby, T.M. An Improved Heat Pulse Method to Measure Low and Reverse Rates of Sap Flow in Woody Plants. *Tree Physiol.* **2001**, *21*, 589–598. [CrossRef]
162. Cohen, Y.; Fuchs, M.; Green, G. Improvement of the Heat Pulse Method for Determining Sap Flow in Trees. *Plant Cell Environ.* **1981**, *4*, 391–397. [CrossRef]
163. Testi, L.; Villalobos, F.J. New Approach for Measuring Low Sap Velocities in Trees. *Agric. For. Meteorol.* **2009**, *149*, 730–734. [CrossRef]
164. Vandegheuchte, M.W.; Steppe, K. Sapflow+: A Four-needle Heat-pulse Sap Flow Sensor Enabling Nonempirical Sap Flux Density and Water Content Measurements. *New Phytol.* **2012**, *196*, 306–317. [CrossRef] [PubMed]
165. López-Bernal, Á.; Testi, L.; Villalobos, F.J. A Single-probe Heat Pulse Method for Estimating Sap Velocity in Trees. *New Phytol.* **2017**, *216*, 321–329. [CrossRef] [PubMed]

166. Pearsall, K.R.; Williams, L.E.; Castorani, S.; Bleby, T.M.; McElrone, A.J. Evaluating the Potential of a Novel Dual Heat-Pulse Sensor to Measure Volumetric Water Use in Grapevines under a Range of Flow Conditions. *Funct. Plant Biol.* **2014**, *41*, 874–883. [[CrossRef](#)] [[PubMed](#)]
167. Nadezhdina, N. Revisiting the Heat Field Deformation (HFD) Method for Measuring Sap Flow. *IForest-Biogeosci. For.* **2018**, *11*, 118. [[CrossRef](#)]
168. Čermák, J.; Kučera, J.; Nadezhdina, N. Sap Flow Measurements with Some Thermodynamic Methods, Flow Integration within Trees and Scaling up from Sample Trees to Entire Forest Stands. *Trees* **2004**, *18*, 529–546. [[CrossRef](#)]
169. Nhean, S.; Isarangkool Na Ayutthaya, S.; Rocheteau, A.; Do, F.C. Multi-Species Test and Calibration of an Improved Transient Thermal Dissipation System of Sap Flow Measurement with a Single Probe. *Tree Physiol.* **2019**, *39*, 1061–1070. [[CrossRef](#)] [[PubMed](#)]
170. Granier, A. Evaluation of Transpiration in a Douglas-Fir Stand by Means of Sap Flow Measurements. *Tree Physiol.* **1987**, *3*, 309–320. [[CrossRef](#)] [[PubMed](#)]
171. Rana, G.; De Lorenzi, F.; Palatella, L.; Martinelli, N.; Ferrara, R.M. Field Scale Recalibration of the Sap Flow Thermal Dissipation Method in a Mediterranean Vineyard. *Agric. For. Meteorol.* **2019**, *269*, 169–179. [[CrossRef](#)]
172. Fuchs, S.; Leuschner, C.; Link, R.; Coners, H.; Schuldt, B. Calibration and Comparison of Thermal Dissipation, Heat Ratio and Heat Field Deformation Sap Flow Probes for Diffuse-Porous Trees. *Agric. For. Meteorol.* **2017**, *244*, 151–161. [[CrossRef](#)]
173. Hernandez-Santana, V.; Fernandes, R.D.; Perez-Arcoiza, A.; Fernández, J.; Garcia, J.; Diaz-Espejo, A. Relationships between Fruit Growth and Oil Accumulation with Simulated Seasonal Dynamics of Leaf Gas Exchange in the Olive Tree. *Agric. For. Meteorol.* **2018**, *256*, 458–469. [[CrossRef](#)]
174. Ferrara, R.M.; Bruno, M.R.; Campi, P.; Camposeo, S.; De Carolis, G.; Gaeta, L.; Martinelli, N.; Mastrorilli, M.; Modugno, A.F.; Mongelli, T.; et al. Water use of a super high-density olive orchard submitted to regulated deficit irrigation in Mediterranean environment over three contrasted years. *Irrig. Sci.* **2024**, *42*, 57–73. [[CrossRef](#)]
175. Saitta, D.; Consoli, S.; Ferlito, F.; Torrisi, B.; Allegra, M.; Longo-Minnolo, G.; Ramirez-Cuesta, J.M.; Vanella, D. Adaptation of Citrus Orchards to Deficit Irrigation Strategies. *Agric. Water Manag.* **2021**, *247*, 106734. [[CrossRef](#)]
176. Abdelfatah, A.; Aranda, X.; Savé, R.; de Herralde, F.; Biel, C. Evaluation of the Response of Maximum Daily Shrinkage in Young Cherry Trees Submitted to Water Stress Cycles in a Greenhouse. *Agric. Water Manag.* **2013**, *118*, 150–158. [[CrossRef](#)]
177. Rawlins, S. Theory for Thermocouple Psychrometers Used to Measure Water Potential in Soil and Plant Samples. *Agric. Meteorol.* **1966**, *3*, 293–310. [[CrossRef](#)]
178. Andraski, B.J.; Scanlon, B.R. 3.2. 3 Thermocouple Psychrometry. In *Methods of Soil Analysis: Part 4 Physical Methods*; John Wiley & Sons: New York, NY, USA, 2002; Volume 5, pp. 609–642.
179. Pérez, E.M.M.; Barrio, J.J.C.; García, T.S.C.; Seijo, X.X.N. Use of Psychrometers in Field Measurements of Plant Material: Accuracy and Handling Difficulties. *Span. J. Agric. Res.* **2011**, *9*, 313–328.
180. Dixon, M.; Tyree, M. A New Stem Hygrometer, Corrected for Temperature Gradients and Calibrated against the Pressure Bomb. *Plant Cell Environ.* **1984**, *7*, 693–697. [[CrossRef](#)]
181. Dainese, R.; de Lopes, B.C.F.L.; Fourcaud, T.; Tarantino, A. Evaluation of Instruments for Monitoring the Soil–Plant Continuum. *Geomech. Energy Environ.* **2022**, *30*, 100256. [[CrossRef](#)]
182. Dainese, R.; de Carvalho Faria Lima Lopes, B.; Tedeschi, G.; Lamarque, L.J.; Delzon, S.; Fourcaud, T.; Tarantino, A. Cross-Validation on Saplings of High-Capacity Tensiometer and Thermocouple Psychrometer for Continuous Monitoring of Xylem Water Potential. *J. Exp. Bot.* **2021**, *73*, 400–412. [[CrossRef](#)] [[PubMed](#)]
183. Kokkotos, E.; Zotos, A.; Patakas, A. The Ecophysiological Response of Olive Trees under Different Fruit Loads. *Life* **2024**, *14*, 128. [[CrossRef](#)]
184. Rodriguez-Dominguez, C.M.; Brodribb, T.J. Declining Root Water Transport Drives Stomatal Closure in Olive under Moderate Water Stress. *New Phytol.* **2020**, *225*, 126–134. [[CrossRef](#)]
185. Prats, K.A.; Fanton, A.C.; Brodersen, C.R.; Furze, M.E. Starch Depletion in the Xylem and Phloem Ray Parenchyma of Grapevine Stems under Drought. *AoB Plants* **2023**, *15*, plad062. [[CrossRef](#)] [[PubMed](#)]
186. Quick, D.; Espino, S.; Morua, M.; Schenk, H. Effects of Thermal Gradients in Sapwood on Stem Psychrometry. In Proceedings of the International Symposium on Sensing Plant Water Status—Methods and Applications in Horticultural Science, Potsdam, Germany, 5–7 October 2016; pp. 23–30.
187. Kanakaraja, P.; Sundar, P.S.; Vaishnavi, N.; Reddy, S.G.K.; Manikanta, G.S. IoT Enabled Advanced Forest Fire Detecting and Monitoring on Ubidots Platform. *Mater. Today Proc.* **2021**, *46*, 3907–3914. [[CrossRef](#)]
188. Niccoli, F.; Pacheco-Solana, A.; Delzon, S.; Kabala, J.P.; Asgharina, S.; Castaldi, S.; Valentini, R.; Battipaglia, G. Effects of Wildfire on Growth, Transpiration and Hydraulic Properties of Pinus Pinaster Aiton Forest. *Dendrochronologia* **2023**, *79*, 126086. [[CrossRef](#)]
189. Laurin, G.V.; Cotrina-Sanchez, A.; Belelli-Marchesini, L.; Tomelleri, E.; Battipaglia, G.; Cocozza, C.; Niccoli, F.; Kabala, J.P.; Gianelle, D.; Vescovo, L. Comparing Ground Below-Canopy and Satellite Spectral Data for an Improved and Integrated Forest Phenology Monitoring System. *Ecol. Indic.* **2024**, *158*, 111328. [[CrossRef](#)]
190. Vasenev, V.I.; Slukovskaya, M.V.; Cheng, Z.; Paltseva, A.A.; Nehls, T.; Korneykova, M.V.; Vasenev, I.I.; Romzaykina, O.N.; Ivashchenko, K.V.; Sarzhanov, D.A. Anthropogenic Soils and Landscapes of European Russia: Summer School from Sea to Sea—A Didactic Prototype. *J. Environ. Qual.* **2021**, *50*, 63–77. [[CrossRef](#)]
191. Fernandes, R.D.M.; Cuevas, M.V.; Diaz-Espejo, A.; Hernandez-Santana, V. Effects of Water Stress on Fruit Growth and Water Relations between Fruits and Leaves in a Hedgerow Olive Orchard. *Agric. Water Manag.* **2018**, *210*, 32–40. [[CrossRef](#)]

192. Greenspan, M.D.; Schultz, H.R.; Matthews, M.A. Field Evaluation of Water Transport in Grape Berries during Water Deficits. *Physiol. Plant.* **1996**, *97*, 55–62. [[CrossRef](#)]
193. Carella, A.; Gianguzzi, G.; Scalisi, A.; Farina, V.; Inglese, P.; Bianco, R.L. Fruit Growth Stage Transitions in Two Mango Cultivars Grown in a Mediterranean Environment. *Plants* **2021**, *10*, 1332. [[CrossRef](#)] [[PubMed](#)]
194. Morandi, B.; Rieger, M.; Grappadelli, L.C. Vascular Flows and Transpiration Affect Peach (*Prunus persica* Batsch.) Fruit Daily Growth. *J. Exp. Bot.* **2007**, *58*, 3941–3947. [[CrossRef](#)]
195. Léchaudel, M.; Lopez-Lauri, F.; Vidal, V.; Sallanon, H.; Joas, J. Response of the Physiological Parameters of Mango Fruit (Transpiration, Water Relations and Antioxidant System) to Its Light and Temperature Environment. *J. Plant Physiol.* **2013**, *170*, 567–576. [[CrossRef](#)]
196. Tukey, L. A Linear Electric Device for Continuous Measurement and Recording of Fruit Enlargement and Contraction. *J. Am. Soc. Hortic. Sci.* **1964**, *84*, 653–660.
197. Higgs, K.; Jones, H. A Microcomputer-Based System for Continuous Measurement and Recording Fruit Diameter in Relation to Environmental Factors. *J. Exp. Bot.* **1984**, *35*, 1646–1655. [[CrossRef](#)]
198. Thalheimer, M. A New Optoelectronic Sensor for Monitoring Fruit or Stem Radial Growth. *Comput. Electron. Agric.* **2016**, *123*, 149–153. [[CrossRef](#)]
199. Morandi, B.; Manfrini, L.; Zibordi, M.; Noferini, M.; Fiori, G.; Grappadelli, L.C. A Low-Cost Device for Accurate and Continuous Measurements of Fruit Diameter. *HortScience* **2007**, *42*, 1380–1382. [[CrossRef](#)]
200. Link, S.; Thiede, M.; Bavel, M. van An Improved Strain-Gauge Device for Continuous Field Measurement of Stem and Fruit Diameter. *J. Exp. Bot.* **1998**, *49*, 1583–1587. [[CrossRef](#)]
201. Grilo, F.; Scalisi, A.; Pernice, F.; Morandi, B.; Lo Bianco, R. Recurrent Deficit Irrigation and Fruit Harvest Affect Tree Water Relations and Fruitlet Growth in ‘Valencia’ Orange. *Eur. J. Hortic. Sci.* **2019**, *84*, 177–187. [[CrossRef](#)]
202. Scalisi, A.; Morandi, B.; Inglese, P.; Bianco, R.L. Cladode Growth Dynamics in *Opuntia Ficus-Indica* under Drought. *Environ. Exp. Bot.* **2016**, *122*, 158–167. [[CrossRef](#)]
203. Scalisi, A.; O’Connell, M.; Turpin, S.; Lo Bianco, R. Diurnal Irrigation Timing Affects Fruit Growth in Late-Ripening Nectarines. In Proceedings of the International Symposium on Precision Management of Orchards and Vineyards, Palermo, Italy, 7–11 October 2019; pp. 61–68.
204. Peppi, L.M.; Zauli, M.; Manfrini, L.; Grappadelli, L.C.; De Marchi, L.; Traverso, P.A. Low-Cost, High-Resolution and No-Manning Distributed Sensing System for the Continuous Monitoring of Fruit Growth in Precision Farming. *Acta IMEKO* **2023**, *12*, 1–11. [[CrossRef](#)]
205. Giovannini, A.; Venturi, M.; Gutiérrez-Gordillo, S.; Manfrini, L.; Corelli-Grappadelli, L.; Morandi, B. Vascular and Transpiration Flows Affecting Apricot (*Prunus armeniaca* L.) Fruit Growth. *Agronomy* **2022**, *12*, 989.
206. Morandi, B.; Manfrini, L.; Losciale, P.; Zibordi, M.; Corelli-Grappadelli, L. Changes in Vascular and Transpiration Flows Affect the Seasonal and Daily Growth of Kiwifruit (*Actinidia deliciosa*) Berry. *Ann. Bot.* **2010**, *105*, 913–923. [[CrossRef](#)]
207. Brüggewirth, M.; Winkler, A.; Knoche, M. Xylem, Phloem, and Transpiration Flows in Developing Sweet Cherry Fruit. *Trees* **2016**, *30*, 1821–1830. [[CrossRef](#)]
208. Morandi, B.; Losciale, P.; Manfrini, L.; Zibordi, M.; Anconelli, S.; Pierpaoli, E.; Grappadelli, L.C. Leaf Gas Exchanges and Water Relations Affect the Daily Patterns of Fruit Growth and Vascular Flows in Abbé Fétel Pear (*Pyrus communis* L.) Trees. *Sci. Hortic.* **2014**, *178*, 106–113. [[CrossRef](#)]
209. Carella, A.; Massenti, R.; Lo Bianco, R. Testing Effects of Vapor Pressure Deficit on Fruit Growth: A Comparative Approach Using Peach, Mango, Olive, Orange, and Loquat. *Front. Plant Sci.* **2023**, *14*, 1294195. [[CrossRef](#)] [[PubMed](#)]
210. Boini, A.; Manfrini, L.; Bortolotti, G.; Corelli-Grappadelli, L.; Morandi, B. Monitoring Fruit Daily Growth Indicates the Onset of Mild Drought Stress in Apple. *Sci. Hortic.* **2019**, *256*, 108520. [[CrossRef](#)]
211. Khosravi, A.; Mohammadi, Z.; Saber, A.; Pourzangbar, A.; Neri, D. Anomaly Detection in Real-Time Continuous Fruit-Based Monitoring of Olive via Extensimeter. 2023, p. 4652476. Available online: <https://ssrn.com/abstract=4652476> (accessed on 12 May 2024).
212. Morandi, B.; Manfrini, L.; Losciale, P.; Zibordi, M.; Corelli-Grappadelli, L. The Positive Effect of Skin Transpiration in Peach Fruit Growth. *J. Plant Physiol.* **2010**, *167*, 1033–1037. [[CrossRef](#)] [[PubMed](#)]
213. Alvino, A.; Marino, S. Remote Sensing for Irrigation of Horticultural Crops. *Horticulturae* **2017**, *3*, 40. [[CrossRef](#)]
214. Semmens, K.A.; Anderson, M.C.; Kustas, W.P.; Gao, F.; Alfieri, J.G.; McKee, L.; Prueger, J.H.; Hain, C.R.; Cammalleri, C.; Yang, Y. Monitoring Daily Evapotranspiration over Two California Vineyards Using Landsat 8 in a Multi-Sensor Data Fusion Approach. *Remote Sens. Environ.* **2016**, *185*, 155–170. [[CrossRef](#)]
215. Messina, G.; Modica, G. Applications of UAV Thermal Imagery in Precision Agriculture: State of the Art and Future Research Outlook. *Remote Sens.* **2020**, *12*, 1491. [[CrossRef](#)]
216. Jones, H.G.; Sirault, X.R. Scaling of Thermal Images at Different Spatial Resolution: The Mixed Pixel Problem. *Agronomy* **2014**, *4*, 380–396. [[CrossRef](#)]
217. Matese, A.; Toscano, P.; Di Gennaro, S.F.; Genesisio, L.; Vaccari, F.P.; Primicerio, J.; Belli, C.; Zaldei, A.; Bianconi, R.; Gioli, B. Intercomparison of UAV, Aircraft and Satellite Remote Sensing Platforms for Precision Viticulture. *Remote Sens.* **2015**, *7*, 2971–2990. [[CrossRef](#)]

218. McCabe, M.F.; Rodell, M.; Alsdorf, D.E.; Miralles, D.G.; Uijlenhoet, R.; Wagner, W.; Lucieer, A.; Houborg, R.; Verhoest, N.E.; Franz, T.E. The Future of Earth Observation in Hydrology. *Hydrol. Earth Syst. Sci.* **2017**, *21*, 3879–3914. [[CrossRef](#)] [[PubMed](#)]
219. Lucieer, A.; Malenovsky, Z.; Veness, T.; Wallace, L. HyperUAS—Imaging Spectroscopy from a Multirotor Unmanned Aircraft System. *J. Field Robot.* **2014**, *31*, 571–590. [[CrossRef](#)]
220. Christiansen, M.P.; Laursen, M.S.; Jørgensen, R.N.; Skovsen, S.; Gislum, R. Designing and Testing a UAV Mapping System for Agricultural Field Surveying. *Sensors* **2017**, *17*, 2703. [[CrossRef](#)]
221. Huang, S.; Tang, L.; Hupy, J.P.; Wang, Y.; Shao, G. A Commentary Review on the Use of Normalized Difference Vegetation Index (NDVI) in the Era of Popular Remote Sensing. *J. For. Res.* **2021**, *32*, 1–6. [[CrossRef](#)]
222. Shao, G. Optical Remote Sensing. *Int. Encycl. Geogr. People Earth Environ. Technol.* **2016**, 1–12. [[CrossRef](#)]
223. Carrasco-Benavides, M.; Antunez-Quilobrán, J.; Baffico-Hernández, A.; Ávila-Sánchez, C.; Ortega-Farías, S.; Espinoza, S.; Gajardo, J.; Mora, M.; Fuentes, S. Performance Assessment of Thermal Infrared Cameras of Different Resolutions to Estimate Tree Water Status from Two Cherry Cultivars: An Alternative to Midday Stem Water Potential and Stomatal Conductance. *Sensors* **2020**, *20*, 3596. [[CrossRef](#)] [[PubMed](#)]
224. Fuentes, S.; De Bei, R.; Pech, J.; Tyerman, S. Computational Water Stress Indices Obtained from Thermal Image Analysis of Grapevine Canopies. *Irrig. Sci.* **2012**, *30*, 523–536. [[CrossRef](#)]
225. Jones, H.G.; Stoll, M.; Santos, T.; de Sousa, C.; Chaves, M.M.; Grant, O.M. Use of Infrared Thermography for Monitoring Stomatal Closure in the Field: Application to Grapevine. *J. Exp. Bot.* **2002**, *53*, 2249–2260. [[CrossRef](#)]
226. Blaya-Ros, P.J.; Blanco, V.; Domingo, R.; Soto-Valles, F.; Torres-Sánchez, R. Feasibility of low-cost thermal imaging for monitoring water stress in young and mature sweet cherry trees. *Appl. Sci.* **2020**, *10*, 5461. [[CrossRef](#)]
227. Blanco, V.; Willsea, N.; Campbell, T.; Howe, O.; Kalcsits, L. Combining Thermal Imaging and Soil Water Content Sensors to Assess Tree Water Status in Pear Trees. *Front. Plant Sci.* **2023**, *14*, 1197437. [[CrossRef](#)]
228. Gonzalez-Dugo, V.; Zarco-Tejada, P.J.; Fereres, E. Applicability and Limitations of Using the Crop Water Stress Index as an Indicator of Water Deficits in Citrus Orchards. *Agric. For. Meteorol.* **2014**, *198*, 94–104. [[CrossRef](#)]
229. Jones, H.G. Use of Infrared Thermometry for Estimation of Stomatal Conductance as a Possible Aid to Irrigation Scheduling. *Agric. For. Meteorol.* **1999**, *95*, 139–149. [[CrossRef](#)]
230. Jackson, R.D.; Kustas, W.P.; Choudhury, B.J. A Reexamination of the Crop Water Stress Index. *Irrig. Sci.* **1988**, *9*, 309–317. [[CrossRef](#)]
231. Agam, N.; Cohen, Y.; Berni, J.; Alchanatis, V.; Kool, D.; Dag, A.; Yermiyahu, U.; Ben-Gal, A. An Insight to the Performance of Crop Water Stress Index for Olive Trees. *Agric. Water Manag.* **2013**, *118*, 79–86. [[CrossRef](#)]
232. Meron, M.; Tsipris, J.; Charitt, D. Remote Mapping of Crop Water Status to Assess Spatial Variability of Crop Stress. In *Precision Agriculture*; Academic Publishers: Berlin, Germany, 2003; pp. 405–410.
233. Möller, M.; Alchanatis, V.; Cohen, Y.; Meron, M.; Tsipris, J.; Naor, A.; Ostrovsky, V.; Sprintsin, M.; Cohen, S. Use of Thermal and Visible Imagery for Estimating Crop Water Status of Irrigated Grapevine. *J. Exp. Bot.* **2007**, *58*, 827–838. [[CrossRef](#)]
234. Irmak, S.; Haman, D.Z.; Bastug, R. Determination of Crop Water Stress Index for Irrigation Timing and Yield Estimation of Corn. *Agron. J.* **2000**, *92*, 1221–1227. [[CrossRef](#)]
235. Gerhards, M.; Schlerf, M.; Mallick, K.; Udelhoven, T. Challenges and Future Perspectives of Multi-/Hyperspectral Thermal Infrared Remote Sensing for Crop Water-Stress Detection: A Review. *Remote Sens.* **2019**, *11*, 1240. [[CrossRef](#)]
236. Apolo-Apolo, O.; Martínez-Guanter, J.; Pérez-Ruiz, M.; Egea, G. Design and Assessment of New Artificial Reference Surfaces for Real Time Monitoring of Crop Water Stress Index in Maize. *Agric. Water Manag.* **2020**, *240*, 106304. [[CrossRef](#)]
237. Park, S.; Ryu, D.; Fuentes, S.; Chung, H.; O'connell, M.; Kim, J. Dependence of CWSI-Based Plant Water Stress Estimation with Diurnal Acquisition Times in a Nectarine Orchard. *Remote Sens.* **2021**, *13*, 2775. [[CrossRef](#)]
238. Araújo-Paredes, C.; Portela, F.; Mendes, S.; Valín, M.I. Using Aerial Thermal Imagery to Evaluate Water Status in *Vitis vinifera* Cv. Loureiro. *Sensors* **2022**, *22*, 8056. [[CrossRef](#)]
239. Bian, J.; Zhang, Z.; Chen, J.; Chen, H.; Cui, C.; Li, X.; Chen, S.; Fu, Q. Simplified Evaluation of Cotton Water Stress Using High Resolution Unmanned Aerial Vehicle Thermal Imagery. *Remote Sens.* **2019**, *11*, 267. [[CrossRef](#)]
240. Cohen, Y.; Alchanatis, V.; Saranga, Y.; Rosenberg, O.; Sela, E.; Bosak, A. Mapping Water Status Based on Aerial Thermal Imagery: Comparison of Methodologies for Upscaling from a Single Leaf to Commercial Fields. *Precis. Agric.* **2017**, *18*, 801–822. [[CrossRef](#)]
241. Caruso, G.; Palai, G.; Tozzini, L.; Gucci, R. Using Visible and Thermal Images by an Unmanned Aerial Vehicle to Monitor the Plant Water Status, Canopy Growth and Yield of Olive Trees (Cvs. Frantoio and Leccino) under Different Irrigation Regimes. *Agronomy* **2022**, *12*, 1904. [[CrossRef](#)]
242. Zhou, H.; Zhou, G.; He, Q.; Zhou, L.; Ji, Y.; Lv, X. Capability of Leaf Water Content and Its Threshold Values in Reflection of Soil-Plant Water Status in Maize during Prolonged Drought. *Ecol. Indic.* **2021**, *124*, 107395. [[CrossRef](#)]
243. Käthner, J.; Ben-Gal, A.; Gebbers, R.; Peeters, A.; Herppich, W.B.; Zude-Sasse, M. Evaluating Spatially Resolved Influence of Soil and Tree Water Status on Quality of European Plum Grown in Semi-Humid Climate. *Front. Plant Sci.* **2017**, *8*, 1053. [[CrossRef](#)] [[PubMed](#)]
244. Zhou, Z.; Majeed, Y.; Naranjo, G.D.; Gambacorta, E.M. Assessment for crop water stress with infrared thermal imagery in precision agriculture: A review and future prospects for deep learning applications. *Comput. Electron. Agric.* **2021**, *182*, 106019. [[CrossRef](#)]

245. Bellvert, J.; Marsal, J.; Girona, J.; Gonzalez-Dugo, V.; Fereres, E.; Ustin, S.L.; Zarco-Tejada, P.J. Airborne Thermal Imagery to Detect the Seasonal Evolution of Crop Water Status in Peach, Nectarine and Saturn Peach Orchards. *Remote Sens.* **2016**, *8*, 39. [CrossRef]
246. Bai, G.; Ge, Y.; Hussain, W.; Baenziger, P.S.; Graef, G. A multi-sensor system for high throughput field phenotyping in soybean and wheat breeding. *Comput. Electron. Agric.* **2016**, *128*, 181–192. [CrossRef]
247. Katz, L.; Ben-Gal, A.; Litaor, M.I.; Naor, A.; Peeters, A.; Goldshtein, E.; Lidor, G.; Keisar, O.; Marzuk, S.; Alchanatis, V. How Sensitive Is Thermal Image-Based Orchard. Water Status Estimation to Canopy Extraction Quality? *Remote Sens.* **2023**, *15*, 1448. [CrossRef]
248. Sánchez-Piñero, M.; Martín-Palomo, M.; Andreu, L.; Moriana, A.; Corell, M. Evaluation of a Simplified Methodology to Estimate the CWSI in Olive Orchards. *Agric. Water Manag.* **2022**, *269*, 107729. [CrossRef]
249. Berni, J.; Zarco-Tejada, P.; Sepulcre-Cantó, G.; Fereres, E.; Villalobos, F. Mapping Canopy Conductance and CWSI in Olive Orchards Using High Resolution Thermal Remote Sensing Imagery. *Remote Sens. Environ.* **2009**, *113*, 2380–2388. [CrossRef]
250. Ben-Gal, A.; Agam, N.; Alchanatis, V.; Cohen, Y.; Yermiyahu, U.; Zipori, I.; Presnov, E.; Sprintsin, M.; Dag, A. Evaluating Water Stress in Irrigated Olives: Correlation of Soil Water Status, Tree Water Status, and Thermal Imagery. *Irrig. Sci.* **2009**, *27*, 367–376. [CrossRef]
251. Gutiérrez-Gordillo, S.; de la Gala González-Santiago, J.; Trigo-Córdoba, E.; Rubio-Casal, A.E.; García-Tejero, I.F.; Egea, G. Monitoring of Emerging Water Stress Situations by Thermal and Vegetation Indices in Different Almond Cultivars. *Agronomy* **2021**, *11*, 1419. [CrossRef]
252. Ramírez-Cuesta, J.M.; Ortuño, M.; Gonzalez-Dugo, V.; Zarco-Tejada, P.J.; Parra, M.; Rubio-Asensio, J.S.; Intrigliolo, D.S. Assessment of Peach Trees Water Status and Leaf Gas Exchange Using On-the-Ground versus Airborne-Based Thermal Imagery. *Agric. Water Manag.* **2022**, *267*, 107628. [CrossRef]
253. Mohamed, A.Z.; Osroosh, Y.; Peters, R.T.; Bates, T.; Campbell, C.S.; Ferrer-Alegre, F. Monitoring Water Status in Apple Trees Using a Sensitive Morning Crop Water Stress Index. *Irrig. Drain.* **2021**, *70*, 27–41. [CrossRef]
254. Jamshidi, S.; Zand-Parsa, S.; Niyogi, D. Assessing Crop Water Stress Index of Citrus Using In-Situ Measurements, Landsat, and Sentinel-2 Data. *Int. J. Remote Sens.* **2021**, *42*, 1893–1916. [CrossRef]
255. Gonzalez-Dugo, V.; Zarco-Tejada, P.; Nicolás, E.; Nortes, P.A.; Alarcón, J.; Intrigliolo, D.S.; Fereres, E. Using High Resolution UAV Thermal Imagery to Assess the Variability in the Water Status of Five Fruit Tree Species within a Commercial Orchard. *Precis. Agric.* **2013**, *14*, 660–678. [CrossRef]
256. Mortazavi, M.; Ehsani, R.; Carpin, S.; Toudeshki, A. Predicting Tree Water Status in Pistachio and Almond Orchards Using Supervised Machine Learning. 2023, preprint submitted. Available online: <https://ssrn.com/abstract=4511076> (accessed on 12 May 2024). [CrossRef]
257. Li, Z.; Wu, H.; Duan, S.; Zhao, W.; Ren, H.; Liu, X.; Leng, P.; Tang, R.; Ye, X.; Zhu, J. Satellite Remote Sensing of Global Land Surface Temperature: Definition, Methods, Products, and Applications. *Rev. Geophys.* **2023**, *61*, e2022RG000777. [CrossRef]
258. Nicolai, B.M.; Beullens, K.; Bobelyn, E.; Peirs, A.; Saeys, W.; Theron, K.I.; Lammertyn, J. Nondestructive Measurement of Fruit and Vegetable Quality by Means of NIR Spectroscopy: A Review. *Postharvest Biol. Technol.* **2007**, *46*, 99–118. [CrossRef]
259. Polesello, A.; Giangiacomo, R.; Dull, G.G. Application of near Infrared Spectrophotometry to the Nondestructive Analysis of Foods: A Review of Experimental Results. *Crit. Rev. Food Sci. Nutr.* **1983**, *18*, 203–230. [CrossRef]
260. Jorge, J.; Vallbé, M.; Soler, J.A. Detection of Irrigation Inhomogeneities in an Olive Grove Using the NDRE Vegetation Index Obtained from UAV Images. *Eur. J. Remote Sens.* **2019**, *52*, 169–177. [CrossRef]
261. Zúñiga Espinoza, C.; Khot, L.R.; Sankaran, S.; Jacoby, P.W. High Resolution Multispectral and Thermal Remote Sensing-Based Water Stress Assessment in Subsurface Irrigated Grapevines. *Remote Sens.* **2017**, *9*, 961. [CrossRef]
262. Pettorelli, N.; Vik, J.O.; Mysterud, A.; Gaillard, J.-M.; Tucker, C.J.; Stenseth, N.C. Using the Satellite-Derived NDVI to Assess Ecological Responses to Environmental Change. *Trends Ecol. Evol.* **2005**, *20*, 503–510. [CrossRef] [PubMed]
263. Jones, H.G.; Vaughan, R.A. *Remote Sensing of Vegetation: Principles, Techniques, and Applications*; Oxford University Press: Oxford, UK, 2010; Volume 223, pp. 229–242.
264. Ballester, C.; Zarco-Tejada, P.J.; Nicolás, E.; Alarcón, J.J.; Fereres, E.; Intrigliolo, D.S.; Gonzalez-Dugo, V. Evaluating the Performance of Xanthophyll, Chlorophyll and Structure-Sensitive Spectral Indices to Detect Water Stress in Five Fruit Tree Species. *Precis. Agric.* **2018**, *19*, 178–193. [CrossRef]
265. Caruso, G.; Palai, G.; Gucci, R.; Priori, S. Remote and Proximal Sensing Techniques for Site-Specific Irrigation Management in the Olive Orchard. *Appl. Sci.* **2022**, *12*, 1309. [CrossRef]
266. Poblete, T.; Ortega-Farías, S.; Moreno, M.A.; Bardeen, M. Artificial Neural Network to Predict Vine Water Status Spatial Variability Using Multispectral Information Obtained from an Unmanned Aerial Vehicle (UAV). *Sensors* **2017**, *17*, 2488. [CrossRef] [PubMed]
267. Baluja, J.; Diago, M.P.; Balda, P.; Zorer, R.; Meggio, F.; Morales, F.; Tardaguila, J. Assessment of Vineyard Water Status Variability by Thermal and Multispectral Imagery Using an Unmanned Aerial Vehicle (UAV). *Irrig. Sci.* **2012**, *30*, 511–522. [CrossRef]
268. Romero, M.; Luo, Y.; Su, B.; Fuentes, S. Vineyard Water Status Estimation Using Multispectral Imagery from an UAV Platform and Machine Learning Algorithms for Irrigation Scheduling Management. *Comput. Electron. Agric.* **2018**, *147*, 109–117. [CrossRef]
269. Zarco-Tejada, P.J.; González-Dugo, V.; Williams, L.; Suarez, L.; Berni, J.A.; Goldhamer, D.; Fereres, E. A PRI-Based Water Stress Index Combining Structural and Chlorophyll Effects: Assessment Using Diurnal Narrow-Band Airborne Imagery and the CWSI Thermal Index. *Remote Sens. Environ.* **2013**, *138*, 38–50. [CrossRef]

270. Rallo, G.; Minacapilli, M.; Ciraolo, G.; Provenzano, G. Detecting Crop Water Status in Mature Olive Groves Using Vegetation Spectral Measurements. *Biosyst. Eng.* **2014**, *128*, 52–68. [CrossRef]
271. Mwinuka, P.R.; Mourice, S.K.; Mbugu, W.B.; Mbilinyi, B.P.; Tumbo, S.D.; Schmitter, P. UAV-based multispectral vegetation indices for assessing the interactive effects of water and nitrogen in irrigated horticultural crops production under tropical sub-humid conditions: A case of African eggplant. *Agric. Water Manag.* **2022**, *266*, 107516. [CrossRef]
272. Tang, Z.; Jin, Y.; Alsina, M.M.; McElrone, A.J.; Bambach, N.; Kustas, W.P. Vine water status mapping with multispectral UAV imagery and machine learning. *Irrig. Sci.* **2022**, *40*, 715–730. [CrossRef]
273. Zhang, L.; Han, W.; Niu, Y.; Chavez, J.L.; Shao, G.; Zhang, H. Evaluating the sensitivity of water stressed maize chlorophyll and structure based on UAV derived vegetation indices. *Comput. Electron. Agric.* **2021**, *185*, 106174. [CrossRef]
274. Stagakis, S.; González-Dugo, V.; Cid, P.; Guillén-Climent, M.L.; Zarco-Tejada, P.J. Monitoring Water Stress and Fruit Quality in an Orange Orchard under Regulated Deficit Irrigation Using Narrow-Band Structural and Physiological Remote Sensing Indices. *ISPRS J. Photogramm. Remote Sens.* **2012**, *71*, 47–61. [CrossRef]
275. Fasiolo, D.T.; Pichierri, A.; Sivilotti, P.; Scalera, L. An analysis of the effects of water regime on grapevine canopy status using a UAV and a mobile robot. *Smart Agric. Technol.* **2023**, *6*, 100344. [CrossRef]
276. Longo-Minnolo, G.; Consoli, S.; Vanella, D.; Guarrera, S.; Manetto, G.; Cerruto, E. Appraising the stem water potential of citrus orchards from UAV-based multispectral imagery. In Proceedings of the 2023 IEEE International Workshop on Metrology for Agriculture and Forestry (MetroAgriFor), Pisa, Italy, 6–8 November 2023; IEEE: Piscataway, NJ, USA, 2023; pp. 120–125.
277. Cohen, Y.; Gogumalla, P.; Bahat, I.; Netzer, Y.; Ben-Gal, A.; Lenski, I.; Michael, Y.; Helman, D. Can Time Series of Multispectral Satellite Images Be Used to Estimate Stem Water Potential in Vineyards? In *Precision Agriculture'19*; Wageningen Academic Publishers: Wageningen, The Netherlands, 2019; pp. 1–5.
278. Lin, Y.; Zhu, Z.; Guo, W.; Sun, Y.; Yang, X.; Kovalsky, V. Continuous Monitoring of Cotton Stem Water Potential Using Sentinel-2 Imagery. *Remote Sens.* **2020**, *12*, 1176. [CrossRef]
279. Boren, E.J.; Boschetti, L. Landsat-8 and Sentinel-2 Canopy Water Content Estimation in Croplands through Radiative Transfer Model Inversion. *Remote Sens.* **2020**, *12*, 2803. [CrossRef]
280. Jiménez-Bello, M.A.; Martínez Alzamora, F.; Carles Campos Alonso, J.; Amparo Martínez Gimeno, M.; Intrigliolo, D.S. Dynamic Citrus Orchards Irrigation Performance Assessment by a Surface Energy Balance Method Using Landsat Imagery. In Proceedings of the 20th EGU General Assembly, EGU2018, Vienna, Austria, 4–13 April 2018; p. 14557.
281. Van Beek, J.; Tits, L.; Somers, B.; Coppin, P. Stem Water Potential Monitoring in Pear Orchards through WorldView-2 Multispectral Imagery. *Remote Sens.* **2013**, *5*, 6647–6666. [CrossRef]
282. Zhang, C.; Marzougui, A.; Sankaran, S. High-Resolution Satellite Imagery Applications in Crop Phenotyping: An Overview. *Comput. Electron. Agric.* **2020**, *175*, 105584. [CrossRef]
283. Schut, A.; Stephens, D.; Stovold, R.; Adams, M.; Craig, R. Improved Wheat Yield and Production Forecasting with a Moisture Stress Index, AVHRR and MODIS Data. *Crop Pasture Sci.* **2009**, *60*, 60–70. [CrossRef]
284. Satellite Imagery Analytics. Available online: <https://www.planet.com/products/planet-imagery/> (accessed on 15 May 2024).
285. Helman, D.; Bahat, I.; Netzer, Y.; Ben-Gal, A.; Alchanatis, V.; Peeters, A.; Cohen, Y. Using Time Series of High-Resolution Planet Satellite Images to Monitor Grapevine Stem Water Potential in Commercial Vineyards. *Remote Sens.* **2018**, *10*, 1615. [CrossRef]
286. Garofalo, S.P.; Giannico, V.; Costanza, L.; Alhaji Ali, S.; Camposeo, S.; Lopriore, G.; Pedrero Salcedo, F.; Vivaldi, G.A. Prediction of Stem Water Potential in Olive Orchards Using High-Resolution Planet Satellite Images and Machine Learning Techniques. *Agronomy* **2024**, *14*, 1. [CrossRef]
287. Gao, B.-C. NDWI—A Normalized Difference Water Index for Remote Sensing of Vegetation Liquid Water from Space. *Remote Sens. Environ.* **1996**, *58*, 257–266. [CrossRef]
288. Rodríguez-Fernández, M.; Fandiño, M.; González, X.P.; Cancela, J.J. Estimation Water Status of the Vineyard by Calculating Multispectral Index from Satellite Images. In Proceedings of the 23rd EGU General Assembly, Online, 19–30 April 2021. [CrossRef]
289. Zhao, T.; Nakano, A.; Iwaski, Y.; Umeda, H. Application of Hyperspectral Imaging for Assessment of Tomato Leaf Water Status in Plant Factories. *Appl. Sci.* **2020**, *10*, 4665. [CrossRef]
290. Pu, R. *Hyperspectral Remote Sensing: Fundamentals and Practices*; CRC Press: Boca Raton, FL, USA, 2017; Volume 1, pp. 4–5.
291. Sahoo, R.N.; Ray, S.; Manjunath, K. Hyperspectral Remote Sensing of Agriculture. *Curr. Sci.* **2015**, *108*, 848–859.
292. Lu, B.; Dao, P.D.; Liu, J.; He, Y.; Shang, J. Recent Advances of Hyperspectral Imaging Technology and Applications in Agriculture. *Remote Sens.* **2020**, *12*, 2659. [CrossRef]
293. Natesan, S.; Armenakis, C.; Benari, G.; Lee, R. Use of UAV-Borne Spectrometer for Land Cover Classification. *Drones* **2018**, *2*, 16. [CrossRef]
294. Gallo, I.; Boschetti, M.; Rehman, A.U.; Candiani, G. Self-Supervised Convolutional Neural Network Learning in a Hybrid Approach Framework to Estimate Chlorophyll and Nitrogen Content of Maize from Hyperspectral Images. *Remote Sens.* **2023**, *15*, 4765. [CrossRef]
295. Rodríguez-Pérez, J.R.; Riaño, D.; Carlisle, E.; Ustin, S.; Smart, D.R. Evaluation of Hyperspectral Reflectance Indexes to Detect Grapevine Water Status in Vineyards. *Am. J. Enol. Vitic.* **2007**, *58*, 302–317. [CrossRef]
296. Jones, C.L.; Weckler, P.R.; Maness, N.O.; Stone, M.L.; Jayasekara, R. Estimating Water Stress in Plants Using Hyperspectral Sensing. *Am. Soc. Agric. Biol. Eng.* **2004**, *1*, 043065.

297. Da Luz, B.R.; Crowley, J.K. Spectral Reflectance and Emissivity Features of Broad Leaf Plants: Prospects for Remote Sensing in the Thermal Infrared (8.0–14.0 Mm). *Remote Sens. Environ.* **2007**, *109*, 393–405. [[CrossRef](#)]
298. Zarco-Tejada, P.J.; González-Dugo, V.; Berni, J.A. Fluorescence, Temperature and Narrow-Band Indices Acquired from a UAV Platform for Water Stress Detection Using a Micro-Hyperspectral Imager and a Thermal Camera. *Remote Sens. Environ.* **2012**, *117*, 322–337. [[CrossRef](#)]
299. Loggenberg, K.; Strever, A.; Greyling, B.; Poona, N. Modelling Water Stress in a Shiraz Vineyard Using Hyperspectral Imaging and Machine Learning. *Remote Sens.* **2018**, *10*, 202. [[CrossRef](#)]
300. Matese, A.; Di Gennaro, S.F.; Orlandi, G.; Gatti, M.; Poni, S. Assessing Grapevine Biophysical Parameters From Unmanned Aerial Vehicles Hyperspectral Imagery. *Front. Plant Sci.* **2022**, *13*, 898722. [[CrossRef](#)]
301. Vasquez, K.; Laroche-Pinel, E.; Partida, G.; Brillante, L. Grapevine water status in a variably irrigated vineyard with NIR hyperspectral imaging from a UAV. In *Precision Agriculture'23*, 1st ed.; Wageningen Academic Publishers: Wageningen, The Netherlands, 2023; pp. 345–350.
302. Gomez-Candon, D.; Labbé, S.; Virlet, N.; Jolivot, A.; Regnard, J.L. High resolution thermal and multispectral UAV imagery for precision assessment of apple tree response to water stress. In *Proceedings of the International Conference on Robotics and Associated High-Technologies and Equipment for Agriculture and Forestry RHEA*; PGM: Madrid, Spain, 2014; Available online: <https://hal.science/hal-01215311> (accessed on 15 May 2024).
303. Blanco, V.; Blaya-Ros, P.J.; Castillo, C.; Soto-Vallés, F.; Torres-Sánchez, R.; Domingo, R. Potential of UAS-Based Remote Sensing for Estimating Tree Water Status and Yield in Sweet Cherry Trees. *Remote Sens.* **2020**, *12*, 2359. [[CrossRef](#)]
304. Zhao, T.; Doll, D.; Wang, D.; Chen, Y. A New Framework for UAV-Based Remote Sensing Data Processing and Its Application in Almond Water Stress Quantification. In *Proceedings of the 2017 International Conference on Unmanned Aircraft Systems (ICUAS)*, Miami, FL, USA, 13–16 June 2017; pp. 1794–1799.
305. Saxton, K.; Rawls, W.; Romberger, J.S.; Papendick, R. Estimating Generalized Soil-water Characteristics from Texture. *Soil. Sci. Soc. Am. J.* **1986**, *50*, 1031–1036. [[CrossRef](#)]
306. Manrique, L.; Jones, C.; Dyke, P. Predicting Soil Water Retention Characteristics from Soil Physical and Chemical Properties. *Commun. Soil. Sci. Plant Anal.* **1991**, *22*, 1847–1860. [[CrossRef](#)]
307. Scott, R.L.; Huxman, T.E.; Barron-Gafford, G.A.; Darrel Jenerette, G.; Young, J.M.; Hamerlynck, E.P. When Vegetation Change Alters Ecosystem Water Availability. *Glob. Chang. Biol.* **2014**, *20*, 2198–2210. [[CrossRef](#)] [[PubMed](#)]
308. Krstić, Đ.; Vujić, S.; Jaćimović, G.; D'Ottavio, P.; Radanović, Z.; Erić, P.; Ćupina, B. The Effect of Cover Crops on Soil Water Balance in Rain-Fed Conditions. *Atmosphere* **2018**, *9*, 492. [[CrossRef](#)]
309. Von Arx, G.; Graf Pannatier, E.; Thimonier, A.; Rebetez, M. Microclimate in Forests with Varying Leaf Area Index and Soil Moisture: Potential Implications for Seedling Establishment in a Changing Climate. *J. Ecol.* **2013**, *101*, 1201–1213. [[CrossRef](#)]
310. Matese, A.; Baraldi, R.; Berton, A.; Cesaraccio, C.; Di Gennaro, S.F.; Duce, P.; Facini, O.; Mameli, M.G.; Piga, A.; Zaldei, A. Estimation of Water Stress in Grapevines Using Proximal and Remote Sensing Methods. *Remote Sens.* **2018**, *10*, 114. [[CrossRef](#)]
311. Gonzalez-Dugo, V.; Testi, L.; Villalobos, F.J.; López-Bernal, A.; Orgaz, F.; Zarco-Tejada, P.J.; Fereres, E. Empirical Validation of the Relationship between the Crop Water Stress Index and Relative Transpiration in Almond Trees. *Agric. For. Meteorol.* **2020**, *292*, 108128. [[CrossRef](#)]
312. Pasqualotto, G.; Carraro, V.; Suarez Huerta, E.; Bono Rosselló, N.; Gilcher, M.; Retzlaff, R.; Garone, E.; Cristofori, V.; Anfodillo, T. Tree-Based Sap Flow Monitoring to Validate the Crop Water Stress Index in Hazelnut. In *Proceedings of the X International Congress on Hazelnut*, Corvallis, OR, USA, 5–9 September 2022; pp. 277–282.

Disclaimer/Publisher's Note: The statements, opinions and data contained in all publications are solely those of the individual author(s) and contributor(s) and not of MDPI and/or the editor(s). MDPI and/or the editor(s) disclaim responsibility for any injury to people or property resulting from any ideas, methods, instructions or products referred to in the content.